Numerical analysis of degenerate connecting orbits for maps

Wolf-Jürgen Beyn,[*] Thorsten Hüls,[*] Jan-Martin Kleinkauf

Fakultät für Mathematik, Universität Bielefeld, Postfach 100131,

D-33501 Bielefeld, Germany.

beyn@mathematik.uni-bielefeld.de, huels@mathematik.uni-bielefeld.de

Yongkui Zou[‡]

Department of Mathematics, Jilin University,

Changchun 130023, P. R. China.

yzou@mail.jl.cn

August 19, 2003

Abstract

This paper contains a survey of numerical methods for connecting orbits in discrete dynamical systems. Special emphasis is put on degenerate cases where either the orbit looses transversality or one of its endpoints looses hyperbolicity. Numerical methods that approximate the connecting orbits by finite orbit sequences are described in detail and theoretical results on the error analysis are provided. For most of the degenerate cases we present examples and numerical results that illustrate the applicability of the methods and the validity of the error estimates.

AMS classification. Primary 65L12. Secondary 58F30, 58F08, 34C45.

Key words and phrases. Degenerate connecting orbit, tangential connecting orbit, dynamical system, numerical approximation.

---

[*]Supported by DFG research group 'Spectral analysis, asymptotic distributions and stochastic dynamics', University of Bielefeld.

[‡]Supported by the VW foundation of Germany, NSFC, Project No. 10071030 of China, the project-sponsored by SRF for ROCS, SEM of China.

Contents

1 Introduction

1.1 Outline of problems

In this paper we survey several papers of our work on the numerical analysis and simulation of degenerate connecting orbits (homoclinic and heteroclinic) for discrete-time dynamical systems. Homoclinic orbits appear in many applications, e.g. in models for economical, physical and biological phenomena, and they may generate rich dynamics. A well-known example occurs near a hyperbolic transversal homoclinic orbit of a diffeomorphism, where the dynamics is equivalent to a horseshoe, and the corresponding map has a chaotic invariant set [Smale, 1963; Palmer, 1988] called a homoclinic tangle [Kuznetsov, 1998]. Transversal homoclinic orbits of ordinary differential equations (ODEs) can lead to chaos under small time-periodic perturbations [Mel'nikov, 1963; Wiggins, 1988]. Homoclinic tangencies are another source of complicated behavior and they are accumulation points of transversal homoclinic and even of other homoclinic tangencies. More precisely, from a quadratic homoclinic tangency of a map there may bifurcate a family of transversal homoclinic orbits and a family of homoclinic tangencies [Palis & Takens, 1993; Arnold et al., 1994].

Mappings arise naturally in the study of continuous time systems. We mention the most frequently occurring examples: the time-T map for an ODE with T-periodic right hand side [Wiggins, 1990], the return map (Poincaré map) associated with a periodic orbit of a flow of an ODE [Hale & Koçak, 1991]. Another source is discretization of an ODE which leads to a family of discrete dynamical systems. It has been proved that hyperbolic homoclinic orbits ([Beyn, 1987; Fiedler & Scheurle, 1996; Zou & Beyn, 2003]) and saddle-node homoclinic orbits ([Zou & Beyn, 1996]), that occur in a continuous system at a specific parameter value, persist in a one-step discretization in a very specific way. They lead to a closed curve of homoclinic orbits on which both transversal and tangential homoclinic orbits occur. Non-diffeomorphism maps are usually induced by the semi-flow of a partial differential equation (PDE) or of a functional differential equation (FDE). In this case the corresponding phase space is an infinite dimensional Banach space. Restricting to center manifolds or inertial manifolds [Mallet-Paret & Sell, 1987], such maps can be reduced to a diffeomorphism on a finite dimensional space.

In the following we describe our terminology and introduce regularity conditions on connecting orbits for maps. This will help in understanding the mechanism that creates the various types of degenerate connecting orbits. In general, a discrete-time dynamical system is characterized by an iteration

$$x_{n+1} = f(x_n, \lambda), \quad x_n \in \mathbb{R}^k,\ n \in \mathbb{Z}, \tag{1.1}$$

where $\lambda \in \mathbb{R}^p$ is a parameter.

We introduce the assumptions used in this paper.

(H1) $f : \mathbb{R}^k \times \mathbb{R}^p \to \mathbb{R}^k$ is C^r-smooth $(r \geq 2)$ and $f(\cdot, \lambda)$ is a diffeomorphism for all $\lambda \in \mathbb{R}^p$.

(H2) $\xi_\pm$ are fixed points of the map $f(\cdot, \lambda)$ at $\lambda = \bar{\lambda}$, i.e. $\xi_\pm = f(\xi_\pm, \bar{\lambda})$.

Let $k_{\pm\kappa},\ \kappa \in \{u, c, s, sc, uc\}$ be the numbers of unstable, center, stable, center-stable and center-unstable eigenvalues (counting multiplicity) of the matrix $f_x(\xi_\pm, \bar{\lambda})$, and let $E^\kappa_\pm,\ \kappa \in \{u, c, s, sc, uc\}$ be the corresponding eigenspaces. By $W^\kappa_\pm,\ \kappa \in \{u, c, s, sc, uc\}$ we denote the corresponding unstable, center, stable, center-stable and center-unstable manifolds of the fixed points $\xi_\pm$ at $\bar{\lambda}$. Notice that the manifolds are generally non-unique if the spectrum contains a center direction. The notations $\xi_\pm(\lambda)$ and $E^\kappa_\pm(\lambda)$ etc. are used whenever the dependence on parameter λ is important.

We consider only bounded orbits of (1.1), so it is useful to work with the Banach space of bounded sequences given by

$$S_{\mathbb{Z}} := \left\{ x_{\mathbb{Z}} = (x_n)_{n \in \mathbb{Z}} : \|x_{\mathbb{Z}}\|_\infty = \sup_{n \in \mathbb{Z}} \|x_n\| < \infty \right\}.$$

A sequence $\bar{x}_{\mathbb{Z}} = (\bar{x}_n)_{n\in\mathbb{Z}}$ is called a **connecting orbit** of the map $f(\cdot,\lambda)$ at $\lambda = \bar{\lambda}$ if $(\bar{x}_{\mathbb{Z}},\bar{\lambda})$ solves the Eq. (1.1) and satisfies $\lim_{n\to\pm\infty}\bar{x}_n = \xi_\pm$. It is called homoclinic if $\xi_+ = \xi_-$ and heteroclinic otherwise. From the geometrical point of view, the connecting orbit lies in the intersection of the unstable manifold W^u_- and the stable manifold W^s_+ if the endpoints $\xi_\pm$ are hyperbolic, see Fig. 1.1 for an illustration of a transversal heteroclinic orbit.

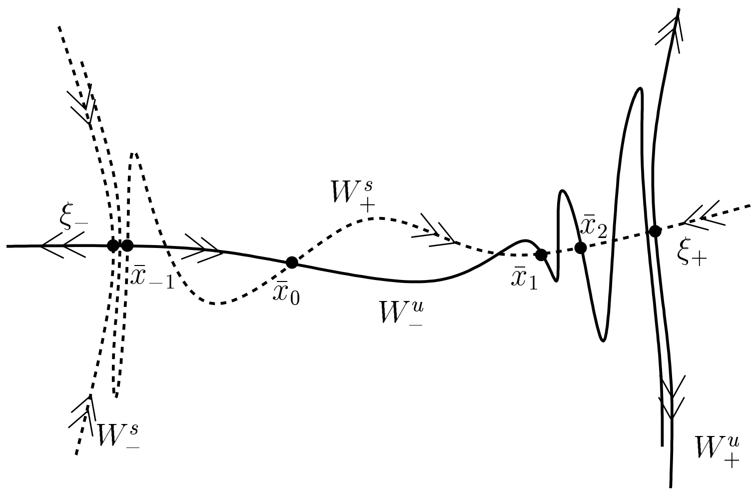

Figure 1.1: Illustration of a transversal heteroclinic orbit.

We call a connecting orbit $\bar{x}_{\mathbb{Z}}$ **regular** at parameter value $\bar{\lambda}$ if it satisfies (H1), (H2) and the following two conditions.

(H3) $k_{\pm c} = 0$, $k_{-u} + k_{+s} = k$.

(H4) The unstable manifold W^u_- and the stable manifold W^s_+ have transversal intersections at $\bar{x}_n$ for all $n \in \mathbb{Z}$.

By the diffeomorphic property the transversality at one point $\bar{x}_0$ is equivalent to transversality at all points $\bar{x}_n$ for $n \in \mathbb{Z}$ (see Fig. 1.1 for an illustration of transversality).

If $k_{\pm c} = 0$, we call the number defined by

$$\mathrm{ind}(x_{\mathbb{Z}}) = k - k_{-u} - k_{+s}$$

index of a hyperbolic connecting orbit $x_{\mathbb{Z}}$. If $k_{-c} + k_{+c} > 0$, the **modified index** is defined as

$$\mathrm{ind}_m(x_{\mathbb{Z}}) = \begin{cases} k - k_{-cu} - k_{+s}, & \text{if the orbit connects center-unstable} \\ & \quad \text{and stable manifold,} \\ k - k_{-u} - k_{+cs}, & \text{if the orbit connects unstable and} \\ & \quad \text{center-stable manifold.} \end{cases}$$

By this definition a regular connecting orbit has index = 0.

Any violation of conditions (H1), (H3), (H4) produces degenerate connecting orbits. In this paper we discuss various possibilities, see Tab. 1.1.

violated condition	degenerate connecting orbit
(H1)	connecting orbit of a non-diffeomorphism
(H3)	connecting orbit with • hyperbolic endpoints ($k_{\pm c} = 0$) ⋆ $\mathrm{ind}(x_{\mathbb{Z}}) > 0$ ⋆ $\mathrm{ind}(x_{\mathbb{Z}}) < 0$ • a singular endpoint ($\mathrm{ind}_m(x_{\mathbb{Z}}) = 0$) ⋆ saddle-fold ⋆ saddle-flip ⋆ saddle-Neimark-Sacker
(H4)	hyperbolic tangential connecting orbit
(H3), (H4)	higher degenerate connecting orbit, e.g. a tangential fold-fold connecting orbit.

Table 1.1: Various degenerate connecting orbits.

Violating (H1) leads to **connecting orbits of non-diffeomorphisms**. There are at least two ways to violate condition (H1). One possibility occurs when the matrix-valued function $f_x(\cdot, \bar{\lambda})$ is not invertible at $\xi_\pm$ or at some points $\bar{x}_n$ along the connecting orbit. Another possibility is that the map $f(\cdot, \bar{\lambda})$ is a non-diffeomorphism defined on an infinite dimensional Banach space. For example, the map $f(\cdot, \bar{\lambda})$ is defined in terms of a time-T map or a return map of the semi-flow of a FDE or a parabolic PDE. In this case the phase space is infinite dimensional and the corresponding map is typically compact and so it cannot have a continuous inverse, even if it is one-to-one. For a detailed discussion of homoclinic orbits of such maps we refer to [Hale & Lin, 1986; Steinlein & Walther, 1990; Lani-Wayda, 1995].

We consider two cases of violating (H3): either $k_{\pm c} = 0$ and $\mathrm{ind}(x_{\mathbb{Z}}) \neq 0$ which generates **hyperbolic connecting orbits with nonzero index** or $k_{+c} + k_{-c} > 0$ and $\mathrm{ind}_m(x_{\mathbb{Z}}) = 0$ which creates **connecting orbits with singular endpoints**.

Case I: $k_{\pm c} = 0$ and $\mathrm{ind}(x_{\mathbb{Z}}) > 0$. The intersection of the manifolds W_-^u and W_+^s may be destroyed by any small perturbation and then the connecting orbit disappears. Such connecting orbits only appear generically in systems with $p = \mathrm{ind}(x_{\mathbb{Z}})$ extra parameters. The numerical computation and error analysis was first discussed in [Beyn & Kleinkauf, 1997; Kleinkauf, 1998c] and was studied in details in [Hüls, 1998]. A hyperbolic heteroclinic orbit of index = 1 will be considered in Sec. 4.

Case II: $k_{\pm c} = 0$ and $\mathrm{ind}(x_{\mathbb{Z}}) < 0$. The intersection of the manifolds W^u_- and W^s_+ produces a nontrivial submanifold of dimension $-\mathrm{ind}(x_{\mathbb{Z}})$. Any point in this submanifold determines a connecting orbit of map (1.1). Therefore, all the corresponding connecting orbits form a continuum.

Some methods for computing high dimensional invariant manifolds can be found in [Krauskopf & Osinga, 1998]. The numerical computation of manifolds of connecting orbits for ODEs discretized from PDEs is presented in [Bai et al., 1993].

Case III: $k_{-c} + k_{+c} > 0$ and $\mathrm{ind}_m(x_{\mathbb{Z}}) = 0$. In this case the unstable (resp. center-unstable) and center-stable (resp. stable) manifolds have a transversal intersection, which produces a connecting orbit with singular endpoint. In this situation some eigenvalues of the Jacobian matrix $f_x(\xi_\pm, \bar{\lambda})$ are on the unit circle. In the simplest case there is precisely one eigenvalue 1 or -1, or there is exactly one pair of complex eigenvalues with unit norm. This gives us the **saddle-fold**, **saddle-flip** and **saddle-Neimark-Sacker connecting orbits**, respectively. Our approximation theory in Sec. 2.1 so far only applies to the first two cases, but in Sec. 2.4 we will treat a numerical example for the last case. For the theory of the first two cases the assumptions (H3) and (H4) are modified to:

(H3') $k_{-c} = 0$, $k_{+c} = 1$ and $k_{-u} + k_{+sc} = k$.

(H4') The invariant manifolds W^u_- and W^{sc}_+ have a transversal intersection at $\bar{x}_0 \in W^{sc}_+ \setminus W^s_+$.

As an example of a connecting orbit with a singular endpoint, we illustrate a saddle-flip connection in Fig. 1.2, where the unstable manifold W^u_- intersects transversally a center-stable manifold W^{cs}_+. In fact, one can show that the transversality is independent of the choice of local center-stable manifolds which are usually not unique.

Violating (H4) provides a **hyperbolic tangential connecting orbit**, which means that the invariant manifolds W^u_- and W^s_+ intersect tangentially at the connecting orbit $x_{\mathbb{Z}}$, cf. Fig. 1.3. In other words, the tangent spaces of the stable and of the unstable manifolds at $\bar{x}_n$ have at least a one dimensional subspace in common. A detailed error analysis and numerical computations can be found in [Kleinkauf, 1998a; Kleinkauf, 1998b; Kleinkauf, 1998c].

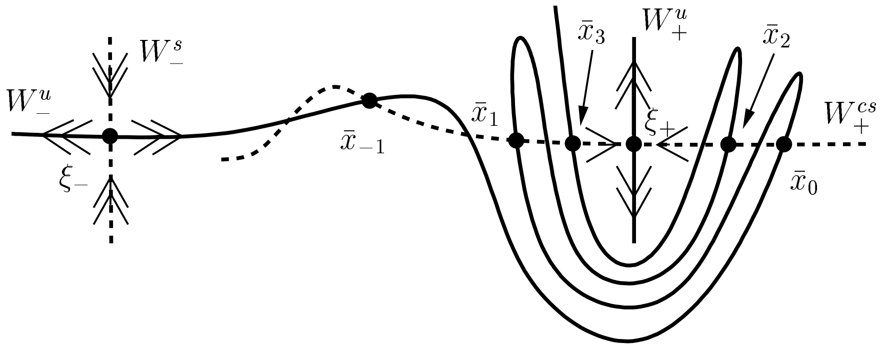

Figure 1.2: An illustration of a saddle-flip heteroclinic for maps.

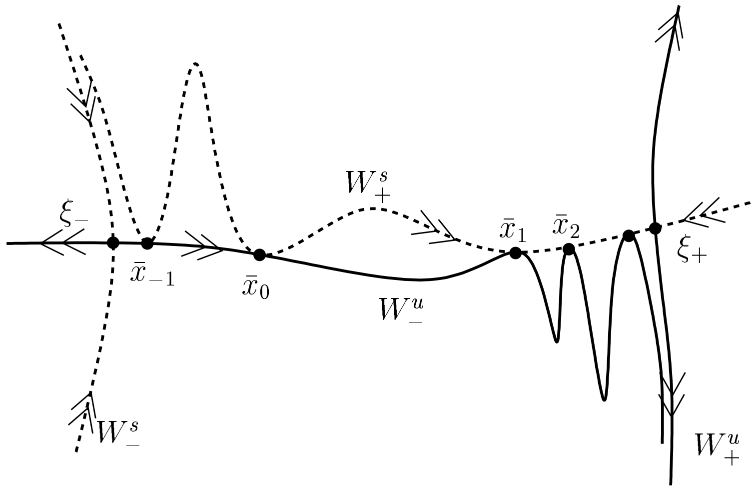

Figure 1.3: Illustration of a tangential heteroclinic orbit.

Violating (H3) and (H4) simultaneously gives a higher order degenerate connecting orbits. As an example we mention a **fold-fold heteroclinic tangency** which will be investigated by numerical computations and simulations in Sec. 3.2.

In this paper, we focus our attention on numerical computation of degenerate connecting orbits and we provide results from an error analysis (without giving proofs for this part). More precisely, we study hyperbolic heteroclinic orbit with index 1, saddle-fold, saddle-flip and saddle-Neimark-Sacker connecting orbits, hyperbolic heteroclinic tangencies and fold-fold heteroclinic tangencies, respectively.

1.2 Numerical approaches

In this subsection we present the numerical method and corresponding error estimates for a regular connecting orbit of a system

$$x_{n+1} = f(x_n), \quad x_n \in \mathbb{R}^k, \quad n \in \mathbb{Z}. \tag{1.2}$$

Guided by the fact that a connecting orbit $\bar{x}_{\mathbb{Z}}$ is a zero of the operator

$$\Gamma : \begin{array}{ccc} S_{\mathbb{Z}} & \to & S_{\mathbb{Z}} \\ x_{\mathbb{Z}} & \mapsto & \Gamma(x_{\mathbb{Z}}) = (x_{n+1} - f(x_n))_{n\in\mathbb{Z}}, \end{array}$$

one can express assumptions (H1)–(H4) in terms of the analytical property that the Frechét derivative

$$\Gamma'(\bar{x}_{\mathbb{Z}}) : S_{\mathbb{Z}} \to S_{\mathbb{Z}}$$

is a linear homeomorphism. In fact, it is shown in [Beyn & Kleinkauf, 1997] that a connecting orbit of the map $f(\cdot)$ that satisfies (H1)–(H3) is regular if and only if this orbit is a regular solution of $\Gamma(x_{\mathbb{Z}}) = 0$.

The fundamentals of numerical methods and of an error analysis for a regular homoclinic orbit in a continuous-time dynamical system were developed in [Beyn, 1990; Doedel & Friedman, 1989; Friedman & Doedel, 1991]. The corresponding results were extended to maps in [Kleinkauf, 1994; Beyn & Kleinkauf, 1997; Hüls, 1998]. For continuous time systems [Schecter, 1993; Sandstede, 1997] consider saddle-node homoclinic orbits and [Champneys & Kuznetsov, 1994] present a systematic approach for approximating codimension-two homoclinic orbits.

In this introduction we summarize some basic results for computing a regular connecting orbit for maps. This will be generalized for degenerate connecting orbits in forthcoming sections.

Let $J = [n_-, n_+] \cap \mathbb{Z}$ be a discrete interval and denote by $\bar{x}_{|J}$ the restriction of the connecting orbit $\bar{x}_{\mathbb{Z}}$ to J. We consider spaces of sequences of finite length

$$S_J = \left\{ x_J = (x_n)_{n\in J} : \|x_J\|_\infty = \sup_{n\in J} \|x_n\| < \infty \right\}.$$

For $|n_\pm|$ large the restriction $\bar{x}_{|J}$ satisfies

$$\begin{array}{l} x_{n+1} - f(x_n) = 0, \quad n = n_-, \cdots, n_+ - 1, \\ x_{n_-} \in W^u_{-\mathrm{loc}} \text{ and } x_{n_+} \in W^s_{+\mathrm{loc}}, \end{array} \tag{1.3}$$

where $W^{u,s}_{\pm\mathrm{loc}}$ represents local invariant manifolds. Our numerical approximation for a connecting orbit will be a finite length orbit $x_J \in S_J$ that satisfies

$$\begin{array}{l} x_{n+1} - f(x_n) = 0, \quad n = n_-, \cdots, n_+ - 1, \\ x_{n_-} \in \tilde{W}^u_{-\mathrm{loc}} \text{ and } x_{n_+} \in \tilde{W}^s_{+\mathrm{loc}}, \end{array} \tag{1.4}$$

where $\tilde{W}^{u,s}_{\pm\text{loc}}$ is some computable approximation of the manifold $W^{u,s}_{\pm\text{loc}}$. Analytically, Eq. (1.4) can be rewritten as

$$\begin{array}{rcll} x_{n+1} - f(x_n) & = & 0, & n = n_-, \cdots, n_+ - 1, \\ b(x_{n_-}, x_{n_+}) & = & 0, & \end{array} \tag{1.5}$$

where $b(x, y) = 0$ represents a boundary condition such that its zeroes satisfy $x \in \tilde{W}^u_{-\text{loc}}$ and $y \in \tilde{W}^s_{+\text{loc}}$, respectively. A well-known choice for the function b is the so-called **projection boundary condition** [Beyn, 1990; Kleinkauf, 1994] where the eigenspace $E^{u,s}_{\pm}$ is used to approximate the local stable and local unstable manifolds, see Fig. 1.4 for a geometrical illustration of the projection boundary condition.

Two problems will be considered

1. Solving the nonlinear system (1.5).
2. Analyzing the solvability of (1.5) and error estimates as $n_\pm \to \infty$.

Equation (1.5) is embedded into a more general parameter-dependent system

$$\begin{array}{rcll} x_{n+1} - f(x_n, \lambda) & = & 0, & n = n_-, \cdots, n_+ - 1, \\ b(x_{n_-}, x_{n_+}, \lambda) & = & 0, & \\ \Phi(x_J, \lambda) & = & 0, & \end{array} \tag{1.6}$$

where Φ is a constraint function which is used to locate some degenerate connecting orbit [Kleinkauf, 1998a; Kleinkauf, 1998b].

To solve Eq. (1.6) we use a Newton type method. During the iteration we have to solve linear equations with the following block structure

$$\mathcal{M} = \begin{bmatrix} M_1 & M_1 & & & & & & M_3 \\ & M_1 & M_1 & & & & & M_3 \\ & & \cdot & \cdot & & & & M_3 \\ & & & \cdot & \cdot & & & M_3 \\ & & & & \cdot & \cdot & & M_3 \\ & & & & & M_1 & M_1 & M_3 \\ M_2 & & & & & & M_2 & M_3 \\ M_4 & M_4 & \cdot & \cdot & \cdot & M_4 & M_4 & M_5 \end{bmatrix}, \tag{1.7}$$

where matrix M_i with the same index i have the same dimension. M_1 is a $k \times k$ matrix determined by the derivatives of the map f with respect to the connecting orbit x_J, M_2 is a $k \times k$ matrix determined by the derivatives of the boundary condition b with respect to (x_{n_-}, x_{n_+}), M_3 is a $k \times p$ matrix determined by the derivatives of the map f with respect to the parameter λ,

M_4 is a $p \times k$ matrix and M_5 is a $p \times p$ matrix determined by derivatives of Φ with respect to (x_J, λ).

A Gaussian elimination method with partly pivoting is used to decompose the matrix $\mathcal{M}$ into an LU-form and keep the block structure unchanged, see [Hager, 1988].

Next we impose a condition on the function b to assure that Eq. (1.5) has a regular solution. For this purpose we assume:

(H5) The function $b(\cdot,\cdot)$ is $C^{\tilde{r}}$-smooth ($\tilde{r} \geq 2$) and satisfies $b(\xi_-, \xi_+) = 0$. The map $B : E^s_- \oplus E^u_+ \to \mathbb{R}^k$ defined by

$$B(x_s, x_u) = D_1 b(\xi_-, \xi_+) x_s + D_2 b(\xi_-, \xi_+) x_u, \quad x_s \in E^s_-, x_u \in E^u_+ \quad (1.8)$$

is nonsingular, where $D_i b$ denotes the derivative of b with respect to the i-th variable.

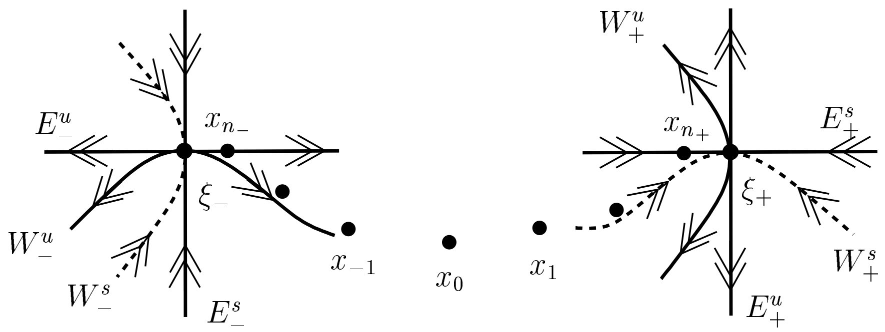

Figure 1.4: Illustration of the projection boundary condition.

Notice that the index=0 condition (H3) guarantees that $E^s_- \oplus E^u_+$ and $\mathbb{R}^k$ have equal dimension. Now we state the approximation theorem for regular connecting orbits (cf. [Beyn & Kleinkauf, 1997; Hüls, 1998]). This theorem provides us with a precise estimate of the approximation error.

Theorem 1.1 [Beyn & Kleinkauf, 1997, Theorem 3.8] *Assume* (H1)–(H5). *Then there exist constants* $\delta, C, N > 0$ *such that the defining system* (1.5) *has a unique solution* x_J *in the ball* $\|x_J - \bar{x}_{|J}\|_\infty \leq \delta$ *for all* $J = [n_-, n_+] \cap \mathbb{Z}$, $|n_\pm| > N$ *and the approximation error satisfies*

$$\|x_J - \bar{x}_{|J}\|_\infty \leq C \|b(\bar{x}_{n_-}, \bar{x}_{n_+})\|. \quad (1.9)$$

There is an extension that states: if $k = k_{-u} + k_{+s} + p$ and an additional nondegeneracy condition with respect to the parameter λ holds, then Theorem 1.1 generalizes to a parameterized system, see [Beyn & Kleinkauf, 1997;

Hüls, 1998]. Assume $\bar{x}_{\mathbb{Z}}(\bar{\lambda})$ is a regular connecting orbit of the map $f(\cdot, \lambda)$ at a parameter $\lambda = \bar{\lambda}$, it follows from the Implicit Function Theorem that a family of λ-dependent regular connecting orbits $\bar{x}_{\mathbb{Z}}(\lambda)$ passes through $\bar{\lambda}$. Applying continuation techniques [Allgower & Georg, 1990] to the system (1.5) allows to trace a family of regular connecting orbits and detect bifurcation points.

It is always a sensitive task to find a starting orbit for solving the defining Eq. (1.5) by an iterative process. In order to approximate a homoclinic orbit, sometimes a simple starting orbit that sets all elements equal to the endpoint but one is sufficient (see [Beyn & Kleinkauf, 1997; Kleinkauf, 1998c]). More sophisticated continuation methods for finding an initial orbit in the continuous time case have been developed in [Friedman & Doedel, 1991]. In general, one can use numerical techniques [Krauskopf & Osinga, 1998] to simulate the invariant manifolds with varying parameter. Then one can try to construct a good starting orbit via the information extracted from these manifolds.

1.3 Structure of the paper

The organization of this paper is as follows. In Sec. 2, we first describe the numerical methods for calculating connecting orbits with singular endpoints and present an error estimate due to [Hüls, 2003]. Then we apply this result to investigate degenerate saddle-fold, saddle-flip and saddle-Neimark-Sacker connecting orbits in three subsections of Sec. 2. In Sec. 3, we study tangential connecting orbits. Examples and error estimates of the numerical method will be presented for a hyperbolic heteroclinic tangency and a fold-fold heteroclinic tangency. Finally, we show some numerical calculations for a hyperbolic heteroclinic orbit with index 1 in Sec. 4.

2 Connecting orbits with singular endpoint

In this section we study the connecting orbits with singular endpoint for a discrete dynamical system

$$x_{n+1} = f(x_n, \lambda), \quad x_n \in \mathbb{R}^k,\ \lambda \in \mathbb{R}^p,\ n \in \mathbb{Z}. \tag{2.1}$$

We consider numerical methods and error estimates for saddle-fold, saddle-flip connecting orbits and present some numerical experiments for the saddle-Neimark-Sacker case.

2.1 A general approximation result

In order to approximate a connecting orbit with singular endpoint we need to compute the connecting orbit, the singular fixed point and the corresponding parameter simultaneously.

First of all, we introduce the numerical method for computing a simple singular fixed point. Assume that the map $f(\cdot,\lambda)$ at $\lambda=\bar{\lambda}$ has a simple fold, flip or Neimark-Sacker fixed point [Kuznetsov, 1998; Govaerts, 2000; Beyn et al., 2002]. We use some defining equation for a singular fixed point ξ_+ and the corresponding parameter $\bar{\lambda}$ (cf. [Seydel, 1979; Seydel, 1988]):

$$\begin{aligned} f(x,\lambda)-x &= 0, \\ \psi(x,\lambda) &= 0, \end{aligned} \tag{2.2}$$

where ψ is a real valued test function for detecting singularities. Detailed definitions and discussions of various test functions can be found in [Beyn et al., 2002, Sec. 3.3].

If the pair $(\xi_+,\bar{\lambda})$ is known we apply the following defining equation to approximate a transversal connecting orbit $\bar{x}_{\mathbb{Z}}$ with singular endpoint at the parameter $\lambda=\bar{\lambda}$

$$\begin{aligned} x_{n+1}-f(x_n,\lambda) &= 0, \quad n=n_-,\cdots,n_+-1, \\ b(x_{n_-},x_{n_+},\lambda) &= 0, \end{aligned} \tag{2.3}$$

where the boundary condition b is properly chosen due to different singularities at ξ_+ (see the following sections).

If the pair $(\xi_+,\bar{\lambda})$ is unknown, we solve the coupled system (2.3) and (2.2) for the combinations $(\bar{x}_J,\xi_+,\bar{\lambda})$.

For simplicity we assume in the following that the fixed point ξ_-, the singular fixed point ξ_+ and the parameter $\bar{\lambda}$ are known.

The linearization of Eq. (2.3) with respect to x_J has the structure of the matrix $\mathcal{M}$ in (1.7) without the matrices M_3, M_4, M_5. Then a Newton type method is implemented to solve the nonlinear Eq. (2.3) at the parameter $\lambda=\bar{\lambda}$.

In the case that the singular fixed point ξ_+ has a simple eigenvalue 1 or -1, there exists a one-dimensional center manifold of the map $f(\cdot,\bar{\lambda})$ at ξ_+. Applying center manifold reduction theory to $f(\cdot,\bar{\lambda})$ we can obtain a one-dimensional reduced system $u_{n+1}=g(u_n)$. Without loss of generality we assume $\xi_+=0$. We make the following assumption.

(H6) The function g of the reduced system has a Taylor expansion

$$g(u)=s_1u+s_2du^{q+1}+\mathcal{O}(u^{q+2}), \quad d>0, \quad u\in\mathbb{R}, \tag{2.4}$$

where $|s_{1,2}|=1$ and in addition $s_1=1$ if q is odd.

For $q = 1$, $s_1 = 1$ we have a fold which attracts points on one side and repels points to the other side.

In case $q = 2$, $s_1 = -1$, $s_2 = 1$ we have a flip point and in case $q = 2$, $s_1 = 1$, $s_2 = -1$ a pitchfork point occurs. In both cases the origin is stable.

A boundary condition b is of **order $(\mathbf{p}_-, \mathbf{p}_+)$** at parameter $\lambda = \bar{\lambda}$ if there exists an integer N such that

$$\|b(\bar{x}_{n_-}, \bar{x}_{n_+}, \bar{\lambda}) - b(\xi_-, \xi_+, \bar{\lambda})\| \leq C(\|\bar{x}_{n_-} - \xi_-\|^{p_-} + \|\bar{x}_{n_+} - \xi_+\|^{p_+}) \quad (2.5)$$

for all $-n_-, n_+ \geq N$.

The orders p_- and p_+ measure the order of contact between the local manifolds $W^{u,s}_{\pm\mathrm{loc}}$ and $\tilde{W}^{u,s}_{\pm\mathrm{loc}}$ in Sec. 1.2.

(H7) The boundary condition b is of order (p_-, p_+) with $p_+ \geq q + 1$.

For approximating hyperbolic connecting orbits we do not need any assumption on the order of the boundary condition, see Theorem 1.1. When analyzing the connecting orbit with a singular endpoint, (H6) and (H7) are needed to obtain the following approximation theorems which are taken from [Hüls, 2003].

Theorem 2.1 [Hüls, 2003, Theorem 4.3] *Assume* (H1), (H2), (H3'), (H4'), (H5)–(H7). *Then there exist constants $\delta, C, N > 0$ such that the defining system* (2.3) *possesses a unique solution x_J at $\lambda = \bar{\lambda}$ in the ball $\|x_J - \bar{x}_{|J}\|_\infty \leq \delta/n_+$ for all $J = [n_-, n_+] \cap \mathbb{Z}$ with $|n_\pm| > N$. The approximation error is given by*

$$\|x_J - \bar{x}_{|J}\|_\infty \leq C\|b(\bar{x}_{n_-}, \bar{x}_{n_+}, \bar{\lambda})\|. \quad (2.6)$$

Corollary 2.2 [Hüls, 2003, Lemma 4.6] *Let the assumptions of* Theorem 2.1 *be satisfied and let $\sigma > 1$ be a number less than the smallest unstable eigenvalue at ξ_- in absolute value, then the following estimate holds*

$$\|x_J - \bar{x}_{|J}\|_\infty \leq C\left(\sigma^{p_- n_-} + \frac{1}{n_+^{(\frac{p_\pm}{q})}}\right).$$

Theorem 2.1 applies to transversal saddle-fold and saddle-flip connecting orbits which will be discussed separately in Sec. 2.2 and 2.3. The saddle-Neimark-Sacker connecting orbit is more complicated and so far we do not know of any error estimates. We present some numerical experiments for such a connecting orbit in Sec. 2.4.

2.2 Saddle-fold connecting orbit

In this subsection we illustrate the estimate given in Corollary 2.2 by numerical computations of saddle-fold connecting orbits for several maps. For the continuous time dynamical system, the associated numerical computations and error estimates for saddle-node homoclinic orbits can be found in [Schecter, 1993; Schecter, 1995; Sandstede, 1997].

Assume ξ_+ is a simple fold point [Govaerts, 2000; Beyn et al., 2002] then we obtain $q = 1$ in Eq. (2.4). Using a projection boundary condition to define the function b in Eq. (2.3) it follows $p_+ \geq 2$. Then Theorem 2.1 can be applied to approximate a transversal saddle-fold connecting orbit by a finite segment, for more details see [Hüls, 2003].

We fix some abbreviations which are used to describe singular points in the following bifurcation diagrams obtained with the program CONTENT, cf. [Kuznetsov & Levitin, 1998]. **BP**: branch point, **Flip**: flip point, **FP**: fold point, **NS**: Neimark-Sacker point, **dashed arrow**: connecting orbit.

Example 1. Consider a Hénon-like map

$$f(x, \lambda) = \begin{pmatrix} 2x_2 \\ x_1 - \lambda - 2x_2 + 4x_2^2 - 8x_2^4 \end{pmatrix}.$$

As the parameter λ varies bifurcation phenomena of fixed points appear, see Fig. 2.1. We have indicated the eigenvalues of the Jacobians by small diagrams. At the parameter value $\bar{\lambda} \approx -0.06475733358165706$ a transversal saddle-fold connecting orbit exists. A numerical connecting orbit together with the corresponding invariant manifolds is plotted in Fig. 2.2. Obviously, the two manifolds intersect transversally.

To approximate the corresponding manifolds numerically, we apply a simple shooting method. We choose a segment of the unstable (stable) subspace in a small neighborhood of the fixed point and iterate with the map f in forward (backward) time to obtain points on the unstable (stable) manifold, respectively. For the center manifold, we apply the same method where the direction of the iteration depends on its stability.

According to [Hüls & Zou, 2001; Hüls, 2003], as $n \to -\infty$ the orbit $\bar{x}_n$ converges to ξ_- with an exponential rate and as $n \to +\infty$ it tends to ξ_+ with a polynomial rate $\mathcal{O}(1/n)$. Noticing $p_+ = 2$ in this example and applying Corollary 2.2 we obtain

$$\|x_J - \bar{x}_{|J}\|_\infty \leq C \frac{1}{n_+^{p_+/q}} = C \frac{1}{n_+^2}. \tag{2.7}$$

Since exact connecting orbit $\bar{x}_\mathbb{Z}$ is unknown, we calculate a very long orbit as a reference connecting orbit $\bar{x}_{[n_-, n_+]}$ by choosing $n_- = -10^3$ and $n_+ = 10^6$.

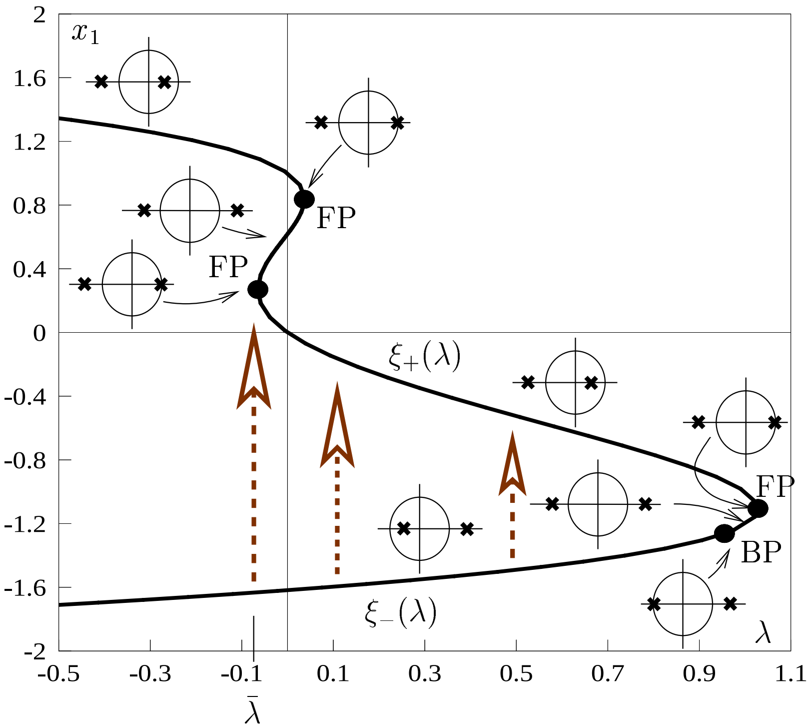

Figure 2.1: Bifurcation diagram of fixed points of f, projected to the (λ, x_1)-space.

Fixing $n_- = -10^3$ and varying $n_+ \le 10^5$ we compute a family of numerical saddle-fold connecting orbits $x_{[n_-,n_+]}$ depending on n_+. The approximation error $\|x_J - \bar{x}_{|J}\|_\infty$ versus n_+ is shown in Fig. 2.3 with both axes in logarithmic scale. According to estimate (2.7) the logarithmic error $\log_{10}(\|x_J - \bar{x}_{|J}\|_\infty)$ should depend linearly on $\log_{10}(n_+)$. The ratios $\frac{-\log_{10}(\|x_J - \bar{x}_{|J}\|_\infty)}{\log_{10}(n_+)}$ tend to 2 as $n_+ \to +\infty$, as demonstrated in the table in Fig. 2.3.

Fig. 2.4 shows the continuation of a hyperbolic heteroclinic orbit towards the saddle-fold heteroclinic orbit. For $\lambda > \bar{\lambda}$ there is a family of hyperbolic heteroclinic orbits $x_{\mathbb{Z}}(\lambda)$ and that terminates at the saddle-fold heteroclinic orbit as λ approaches $\bar{\lambda}$ (see also Fig. 2.1).

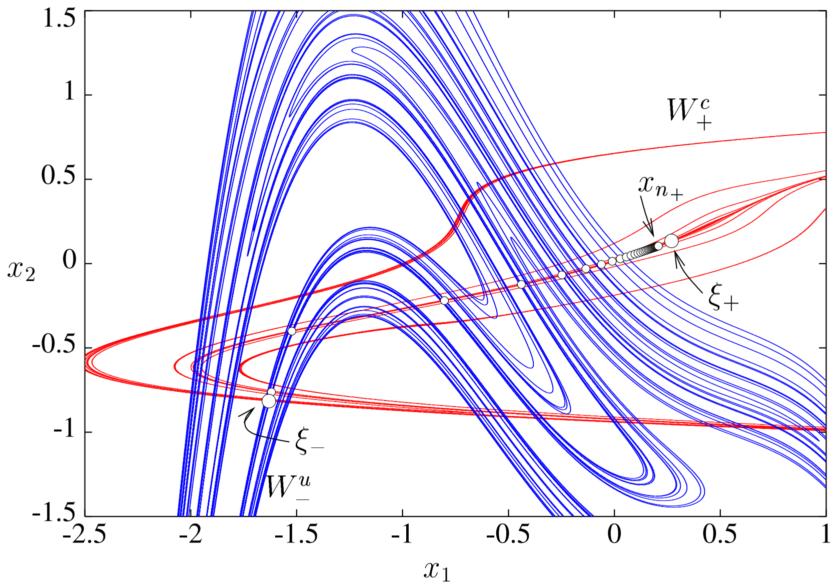

Figure 2.2: A heteroclinic orbit connecting the saddle ξ_- (unstable manifold in blue) to the fold ξ_+ (center manifold in red).

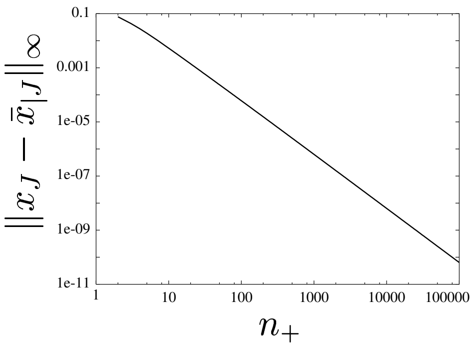

n_+	$\dfrac{-\log_{10}\left(\|x_J - \bar{x}_{\|J}\|_\infty\right)}{\log_{10}(n_+)}$
10^1	2.275663
10^2	2.108344
10^3	2.066127
10^4	2.048710
10^5	2.038883

Figure 2.3: Global approximation errors as a function of n_+ (bi-logarithmic scale) and estimated polynomial rates.

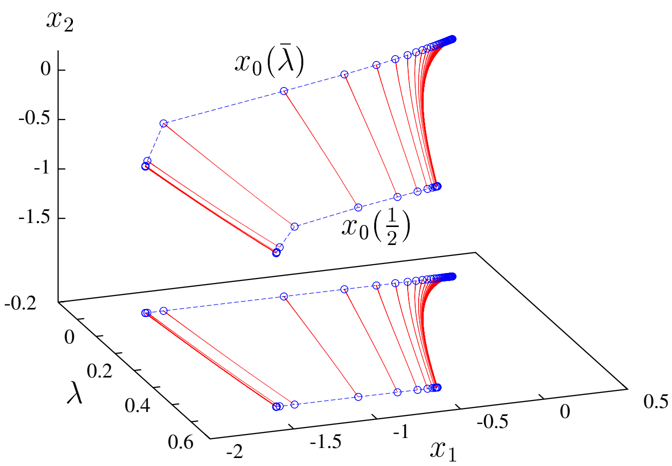

Figure 2.4: Continuation of connecting orbits (red) of length $n_- = -10$, $n_+ = 30$ for $f(\cdot, \lambda)$ starting at $\lambda = \frac{1}{2}$. The initial and final orbits are shown in blue and a projection onto the (x_1, λ) space is displayed.

Example 2. In this example we study transversal fold-fold connecting orbits of maps determined by discretizing the so called DC Josephson Junction equation [Friedman & Doedel, 1993]

$$\dot{x} = h(x, \lambda_1, \lambda_2) = (-x_2, \frac{1}{\lambda_2}(x_2 + \sin(x_1) - \lambda_1))^T. \tag{2.8}$$

Note that the orbit to be calculated converges with an exponential rate to one fixed point while the convergence towards the other fixed point has a polynomial rate. In fact, Theorem 2.1 can be modified to apply to this case as well.

First consider the explicit Euler method with step-size ε

$$x_{n+1} = x_n - \varepsilon h(x_n, \lambda_1, \lambda_2). \tag{2.9}$$

This map has two families of fixed points $\xi_- = (\arcsin(\lambda_1), 0)$ and $\xi_+ = (\pi - \arcsin(\lambda_1), 0)$ which are independent of the parameters ε and λ_2. At $\lambda_1 = -1$ these fixed points have a simple eigenvalue 1, thus they are fold points. Fixing $\bar\lambda_2 \approx 0.8337412881$ and varying λ_1, the bifurcation diagram of these fixed points is shown in Fig. 2.5. At the parameter $\varepsilon = 0.5$, $\bar\lambda_1 = -1$

we find a connecting orbit lying on the intersection of the unstable manifold W_-^u and the center manifold W_+^c, see Fig. 2.6. Parts of the connecting orbit and parts of the invariant manifolds W_-^u, W_+^c are plotted in Fig. 2.7 to show the transversality of this fold-fold connecting orbit.

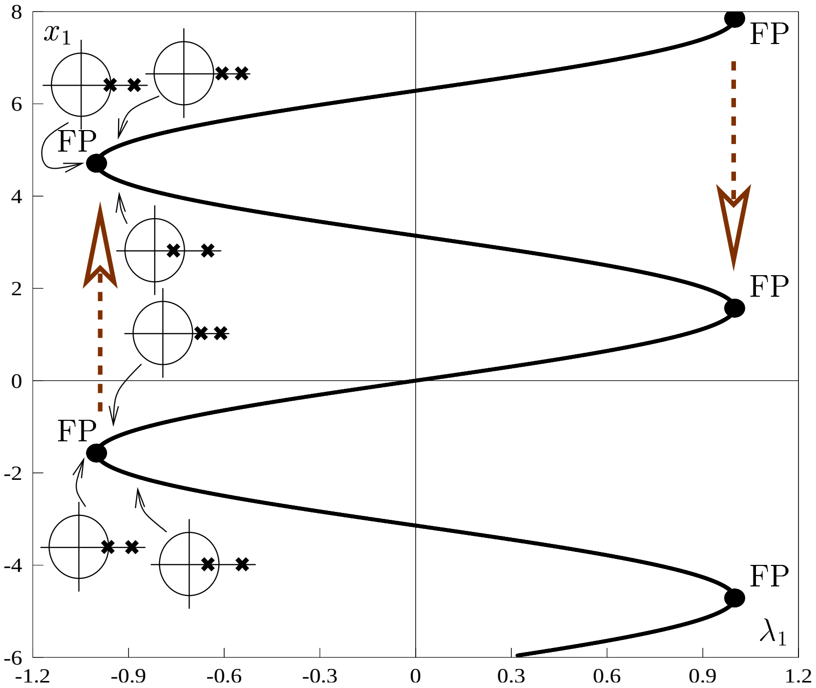

Figure 2.5: Bifurcation diagram of fixed points of the explicit Euler map (2.9), projected in the (x_1, λ_1)-space.

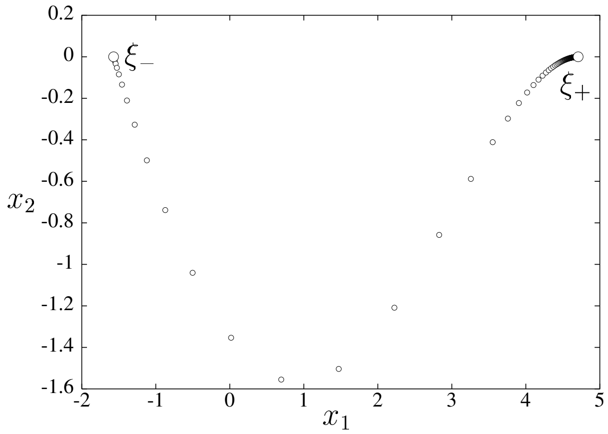

Figure 2.6: An approximation of a fold-fold heteroclinic orbit.

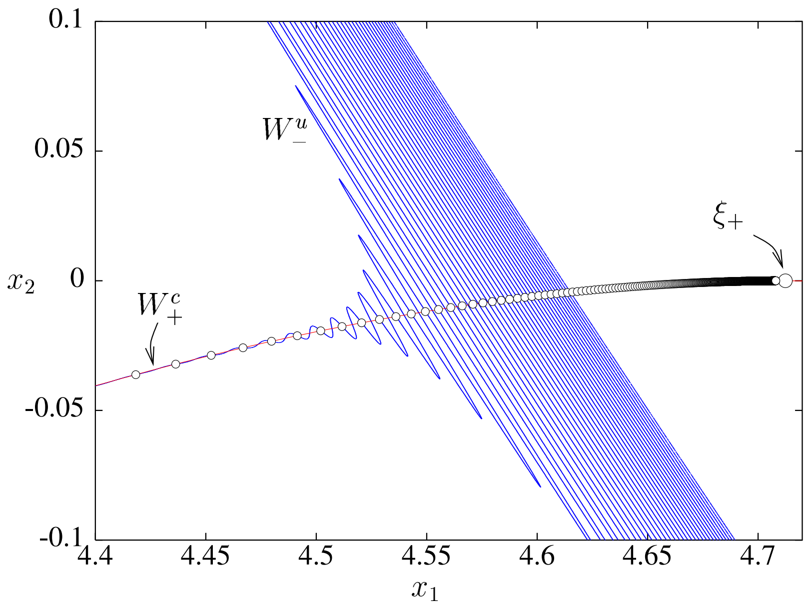

Figure 2.7: Transversal intersection of W_+^c (red) and W_-^u (blue) and parts of the fold-fold heteroclinic orbit.

Second, consider the implicit midpoint Euler method

$$\frac{x_{n+1} - x_n}{\varepsilon} = h\left(\frac{x_{n+1} + x_n}{2}, \lambda_1, \lambda_2\right).$$

This equation is equivalent to

$$F(x_{n+1}, x_n, \lambda_1, \lambda_2, \varepsilon) := x_{n+1} - x_n - \varepsilon h\left(\frac{x_{n+1} + x_n}{2}, \lambda_1, \lambda_2\right) = 0. \quad (2.10)$$

We obtained a discrete fold-fold connecting orbit at $\varepsilon = 0.5$, $\tilde{\lambda}_1 = 1$ and at $\tilde{\lambda}_2 \approx 0.6848193427789787$. This heteroclinic orbit connects the two fold points at the right side of Fig. 2.5.

We plot the whole branch of connecting orbits in an (x_1, x_2, λ_2)-diagram (see Fig. 2.8) and obtain a so called heteroclinic crown. The initial orbit has been marked in blue. Moving λ_2 up and down yields the single orbits. In the hyperbolic case this phenomenon is proved in [Zou & Beyn, 2003] but we do not know of any proof in the current situation.

Remark 2.3 *In order to approximate a discrete degenerate heteroclinic orbit for the implicit* Eq. (2.10)*, we set up a defining equation directly in terms* *of the function F without computing the map $f(\cdot, \lambda_1, \lambda_2, \varepsilon)$ in a preliminary step. Then we get the system*

$$\begin{array}{rcl} F(x_{n+1}, x_n, \lambda_1, \lambda_2, \varepsilon) & = & 0, \quad n = n_-, \cdots, n_+ - 1, \\ b(x_{n_-}, x_{n_+}, \lambda_1, \lambda_2, \varepsilon) & = & 0, \end{array} \tag{2.11}$$

where b represents a boundary condition. The linearization of Eq. (2.11) *with respect to x_J has the form of the matrix $\mathcal{M}$ in* (1.7) *without the matrices $M_{3,4,5}$ and Newton's iterative method can be applied to solve the nonlinear* Eq. (2.11).

Dealing with implicit equations is a general problem and could have easily been done throughout the whole paper for all cases of degenerate orbits. However, for ease of reading we did not rewrite all the methods for implicitly defined mappings.

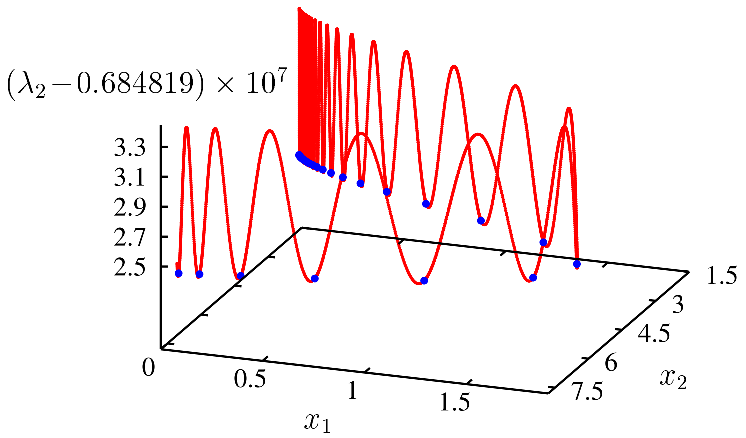

Figure 2.8: Continuation of the fold-fold connecting orbits (red) for the implicit midpoint Euler method with respect to the parameter λ_2 (heteroclinic crown). Initial orbit marked in blue.

2.3 Saddle-flip connecting orbit

In this subsection we present some numerical results on computing saddle-flip connecting orbits for maps. Error estimates for this case are provided in Theorem 2.1. The restriction to a center manifold of a system having a flip fixed point at 0 is of the form (2.4) where $s_1 = -1$ and $q = 2$. Therefore, condition (H7) requires $p_+ \geq 3$ for the order of the boundary condition. This means we need a high order boundary condition to approximate a saddle-flip connecting orbit.

Consider a Hénon-like map

$$f(x,\lambda) = \begin{pmatrix} \left(\frac{1}{2} - \lambda\right) x_1 + x_1^3 + \frac{2}{5}x_1^4 + x_2 \\ \frac{3}{2}x_1 \end{pmatrix}. \tag{2.12}$$

For any $\lambda \in (-0.5, 0.5)$ there are two families of fixed points $\xi_+(\lambda) \equiv 0$ and $\xi_-(\lambda)$. At $\lambda = 0$ the fixed point ξ_+ undergoes a flip bifurcation and a family of period–2 orbits appears for $\lambda > 0$. See Fig. 2.9 for a bifurcation diagram.

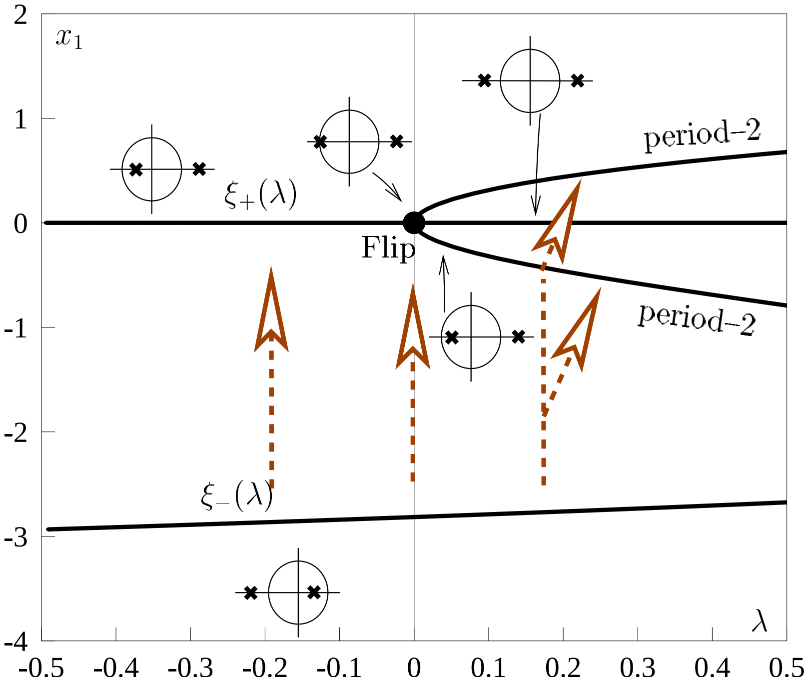

Figure 2.9: Detail of bifurcation diagram of fixed points of f, projected to the (λ, x_1)-space.

We can show that in this example the tangent space E_+^c approximates the center manifold W_+^c to the second order due to the missing x_1^2 term. Therefore, the projection boundary condition has the order $p_+ = 3$ and Theorem 2.1 applies also to this example.

Implementing the numerical method (2.3) we obtain a transversal saddle-flip connecting orbit at the parameter $\bar{\lambda} = 0$. This is shown in Fig. 2.10 together with the corresponding unstable and center manifolds. From this picture, we clearly see the transversal intersection of the invariant manifolds and also observe the polynomial rate of convergence of the connecting orbit towards the flip point ξ_+. An explicit formula for this transition of rates is derived for a model function in [Hüls, 2003].

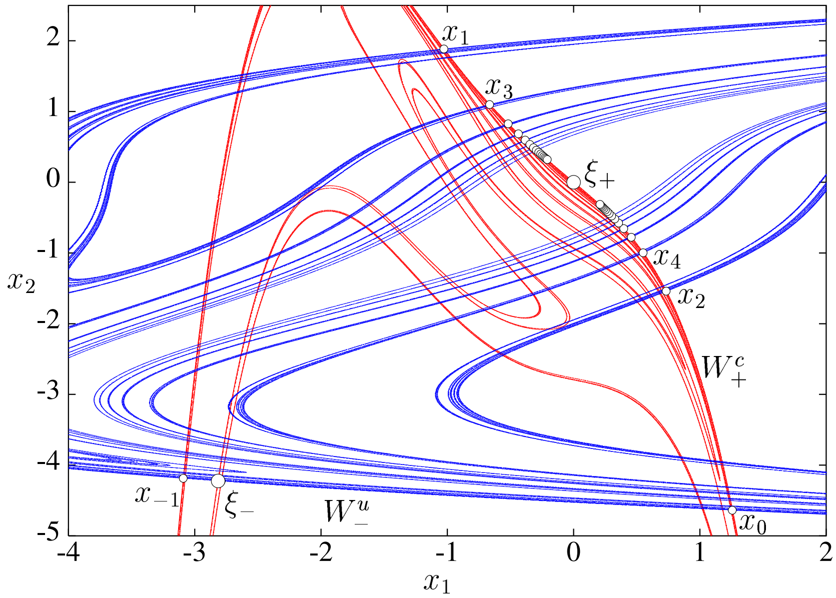

Figure 2.10: Transversal intersection of W^c_+ (red) and W^u_- (blue) and a saddle-flip heteroclinic orbit.

We start the continuation towards the saddle-flip connection at a saddle-saddle connecting orbit at $\lambda = -0.5$. This orbit becomes singular at $\lambda = 0$ and the rate of convergence becomes polynomial. For $\lambda > 0$ we get an orbit converging towards the period-2 orbit with an exponential rate, see Fig. 2.11

In order to illustrate the estimate for the approximation error

$$\|x_J - \bar{x}_{|J}\|_\infty \leq C \frac{1}{n_+^{p_+/q}} = C \frac{1}{n_+^{3/2}}, \tag{2.13}$$

we compute a very long connecting orbit $\bar{x}_{|J}$ with $J = [-10^3, 10^6]$ as a reference orbit. Fixing $n_- = -10^3$ and varying $n_+ \leq 10^5$ we obtain a family of numerical saddle-flip connecting orbits $x_{[n_-, n_+]}$ depending on n_+. The errors between x_J and $\bar{x}_{|J}$ is shown in Fig. 2.12 with both axes plotted in logarithmic scale. It follows from the estimate (2.13) that the ratios $\frac{-\log_{10}\|x_J-\bar{x}_{|J}\|_\infty}{\log_{10}(n_+)}$ converge to $p_+/q = 3/2$ as shown in the table in Fig. 2.12.

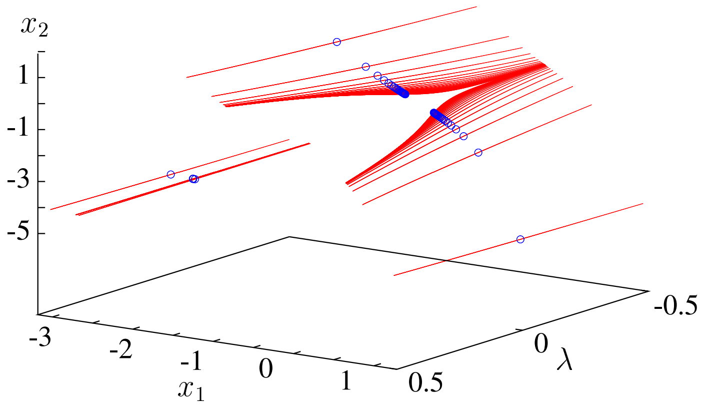

Figure 2.11: Continuation of connecting orbits (red) from saddle-saddle type to saddle-period-2 type via a saddle-flip type (blue).

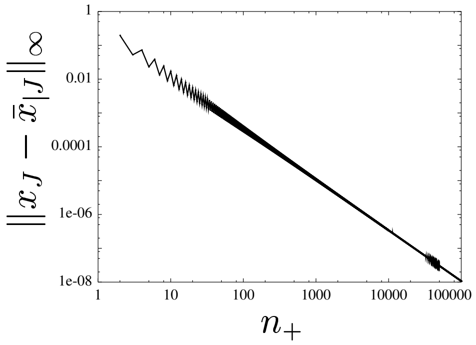

n_+	$\frac{-\log_{10}\left(\|x_J - \bar{x}_{\vert J}\|_\infty\right)}{\log_{10}(n_+)}$
10^1	1.768373
10^2	1.691385
10^3	1.647903
10^4	1.616169
10^5	1.594269

Figure 2.12: Global approximation errors as a function of n_+ (bi-logarithmic scale) and estimated polynomial rates.

2.4 Saddle-Neimark-Sacker connecting orbit

In this subsection we show numerical computations of a transversal saddle-Neimark-Sacker connecting orbit. For differential equations this corresponds to the so called Shilnikov-Hopf case for which numerical experiments are presented in [Champneys & Kuznetsov, 1994]. To our knowledge, there are no theoretical results on error estimates for these connecting orbits in both continuous and discrete time dynamical systems.

Consider an extended Hénon map

$$f(x,y,z) = \begin{pmatrix} \lambda_1(y+z)\left(y+z-2+\frac{1}{2\lambda_1}\right) \\ \frac{1}{4}z^2+\frac{3}{4}z \\ \lambda_2(x+y^3)\left(x-1+(y-1)^3+\frac{1}{2\lambda_2}\right) \end{pmatrix}, \quad \lambda_{1,2} \neq 0 \qquad (2.14)$$

which has two families of fixed points independent of λ_1 and λ_2:

$$\xi_- = (0,0,0) \quad \text{and} \quad \xi_+ = (1,1,1).$$

This map exhibits rich bifurcation phenomena of fixed points. For $\lambda_2 = 0.1$ fixed and λ_1 varying, we obtain the bifurcation diagram shown in Fig. 2.13.

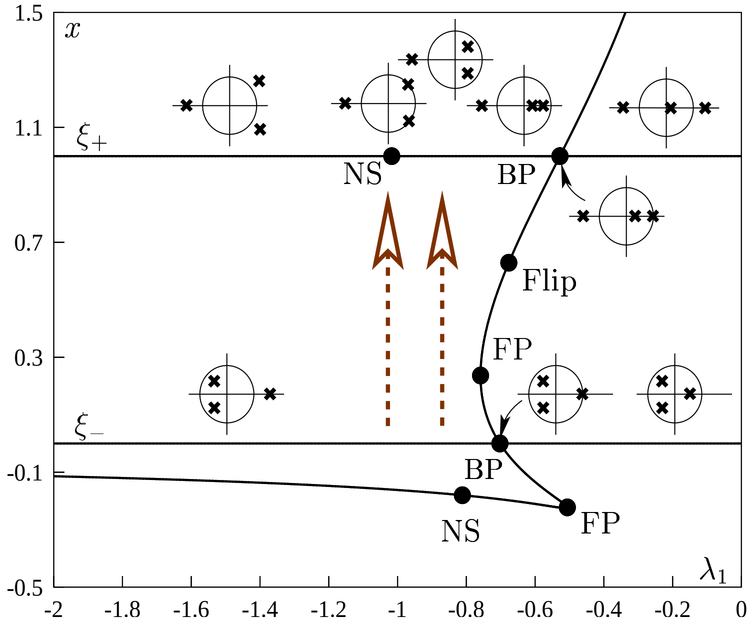

Figure 2.13: Bifurcation diagram of fixed points of f, projected to the (λ_1, x)-space.

At $\bar{\lambda}_1 \approx -1.016928$ we find a saddle-Neimark-Sacker connecting orbit by numerical computation, see Fig. 2.14. This connecting orbit locates at the intersection of the one-dimensional unstable manifold W_-^u and a two-dimensional center manifold W_+^c. We project parts of the numerical connecting orbit together with parts of the one-dimensional unstable manifold W_-^u to the (x, z)-plane (Fig. 2.15). The picture clearly shows the transversality of this saddle-Neimark-Sacker orbit.

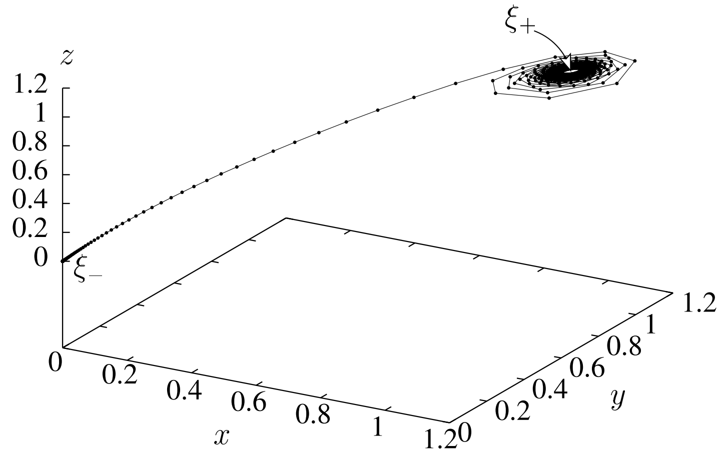

Figure 2.14: A numerical computed saddle-Neimark-Sacker connecting orbit.

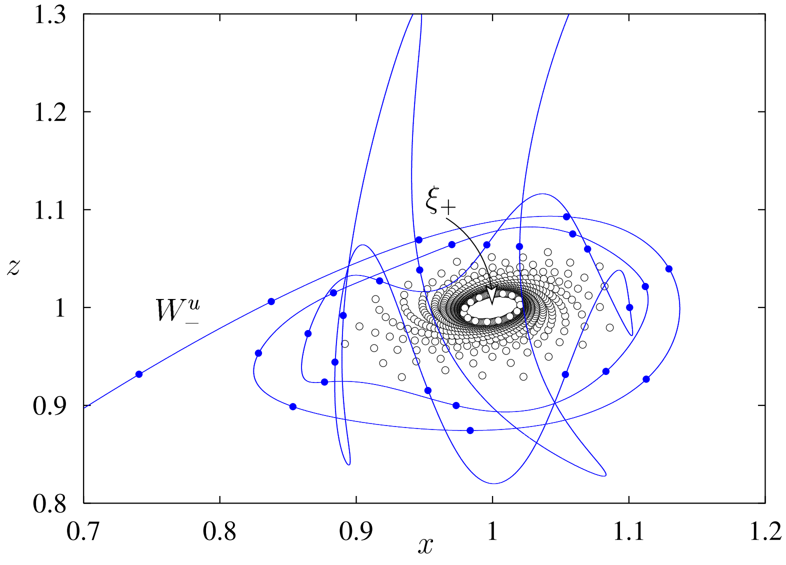

Figure 2.15: Illustration of the transversality of a saddle-Neimark-Sacker connecting orbit projected to (x, z)-plane.

For $\lambda_1 > \bar{\lambda}_1$ there exists a family of hyperbolic heteroclinic orbits and they converge to the saddle-Neimark-Sacker heteroclinic orbit as $\lambda_1 \to \bar{\lambda}_1$ (cf. Fig. 2.13). The continuation of a hyperbolic connecting orbit towards a saddle-Neimark-Sacker connecting orbit with respect to the parameter λ_1 is shown in Fig. 2.16. When λ_1 decreases to $\bar{\lambda}_1$, the rate of convergence of the connecting orbit towards the fixed point ξ_+ changes gradually from an exponential rate to a polynomial rate.

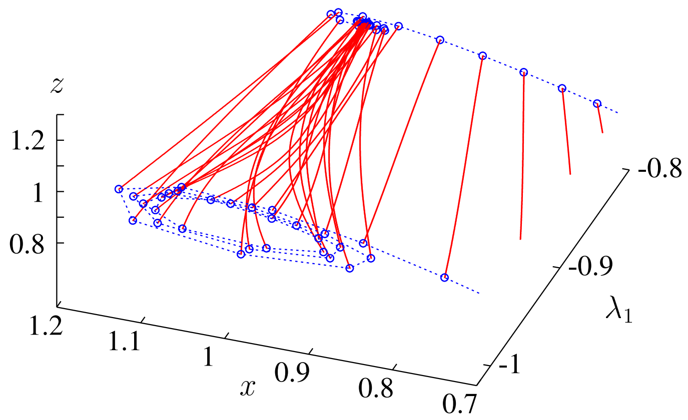

Figure 2.16: Continuation of connecting orbits (red) of length $n_- = -1000$, $n_+ = 30$ with respect to the parameter λ_1. Initial and final orbits are shown as open circles (blue).

Theorem 2.1 does not apply to saddle-Neimark-Sacker connecting orbits and we do not have error estimate for approximating such orbits. But our numerical computations illustrate the approximation error and lead to some conjecture.

At the Neimark-Sacker fixed point ξ_+, a pair of complex eigenvalues $e^{\pm i\theta}$ with $\theta \approx 0.83515485242439$ exists. Applying center manifold theory, the system (2.14) can be reduced to a planar system with variable $(x_1, x_2) \in \mathbb{R}^2$. According to [Kuznetsov, 1998, Theorem 4.5] this reduced system can be transformed into normal form written in polar coordinates (ρ, φ) as

$$f(\rho, \varphi) = \begin{pmatrix} \rho - d\rho^3 + \rho^4 g_1(\rho, \varphi) \\ \theta + \varphi + \rho^2 g_2(\rho, \varphi) \end{pmatrix}, \tag{2.15}$$

where $d > 0$ is a constant and $g_{1,2}$ are smooth bounded functions for ρ small and all $\varphi \in \mathbb{R}$.

Eq. (2.15) shows that all Neimark-Sacker connecting orbits $(\bar{x}_n)_{n\in\mathbb{Z}}$ converge in a spiral manner to the fixed point ξ_+ with a polynomial rate $\mathcal{O}(1/n^{\frac{1}{2}})$ as $n \to +\infty$. We use projection boundary condition to approximate the saddle-Neimark-Sacker connecting orbit which gives $p_+ = 2$ for Eq. (2.5).

To illustrate the errors we use again a very long reference orbit with $J = [-10^3, 10^5]$. Fixing $n_- = -10^3$ and varying $n_+ \le 10^4$ we obtain a family of numerical saddle-Neimark-Sacker connecting orbits $x_{[n_-,n_+]}$ depending on n_+. The error between x_J and $\bar{x}_{|J}$ is shown in Fig. 2.17 with both axes plotted in logarithmic scale. The behaviors of the global approximation errors plotted in Fig. 2.17 suggests that also in this case an error estimate of the following form holds

$$\|x_J - \bar{x}_{|J}\|_\infty \le |b(\bar{x}_{n_-}, \bar{x}_{n_+})| \le C\frac{1}{n_+^{p+/q}}.$$

A look at the ratios $\frac{-\log_{10}\|x_J - \bar{x}_{|J}\|_\infty}{\log_{10}(n_+)}$ suggest that this estimate holds with $n_+ = q = 2$.

However, in contrast to Figs. 2.3 and 2.12 oscillations occur in Fig. 2.17. These oscillations observed in Fig. 2.17 are probably due to the errors caused by the φ iteration of (2.15).

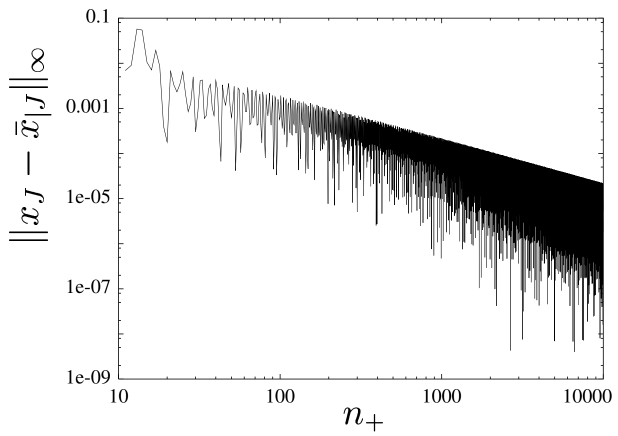

Figure 2.17: Global approximation errors as a function of n_+, plotted in bi-logarithmic scale.

3 Tangential connecting orbits

In this section we study tangential connecting orbits for parameter-dependent maps

$$x_{n+1} = f(x_n, \lambda), \quad x_n \in \mathbb{R}^k,\ \lambda \in \mathbb{R}^p,\ n \in \mathbb{Z}. \tag{3.1}$$

In Sec. 3.1 we consider hyperbolic heteroclinic tangencies and in Sec. 3.2 a fold-fold heteroclinic tangency.

3.1 Tangential hyperbolic connecting orbit

In this subsection we introduce numerical methods and error estimates for a nondegenerate hyperbolic heteroclinic tangency of Eq. (3.1) and present some numerical experiments. For a detailed analysis of this case we refer to [Kleinkauf, 1998a; Kleinkauf, 1998b; Kleinkauf, 1998c].

At a fixed parameter $\lambda = \bar{\lambda}$ we call a connecting orbit $\bar{x}_{\mathbb{Z}}$ **t-tangential** if the tangent spaces to the manifolds W_-^u and W_+^s at $\bar{x}_0$ have a common subspace of dimension t, see Fig. 1.3 for an illustration of a 1-tangential heteroclinic orbit. In case $t = 0$ we have a transversal connecting orbit (cf. Fig. 1.1). If in addition the assumptions (H1)–(H3) hold, the t-tangential connecting orbit is called **nondegenerate**. A 1-tangential connecting orbit is called **quadratic** if the manifolds W_-^u and W_+^s have a quadratic contact at $\bar{x}_0$ (see [Newhouse et al., 1983] for this notion).

The geometrical notion of a t-tangency can be equivalently expressed in terms of the operator

$$\Gamma : \begin{array}{rcl} S_{\mathbb{Z}} \times \mathbb{R}^p & \to & S_{\mathbb{Z}} \\ (x_{\mathbb{Z}}, \lambda) & \mapsto & \Gamma(x_{\mathbb{Z}}, \lambda) = (x_{n+1} - f(x_n, \lambda))_{n \in \mathbb{Z}}. \end{array} \tag{3.2}$$

In [Kleinkauf, 1998a] it is shown that $\bar{x}_{\mathbb{Z}}$ is t-tangential at $\lambda = \bar{\lambda}$ if and only if the Frechét derivative of Γ with respect to $x_{\mathbb{Z}}$ at $(\bar{x}_{\mathbb{Z}}, \bar{\lambda})$

$$\Gamma'_{x_{\mathbb{Z}}}(\bar{x}_{\mathbb{Z}}, \bar{\lambda}) : S_{\mathbb{Z}} \to S_{\mathbb{Z}}$$

has a t-dimensional nullspace. Moreover a quadratic 1-tangential connecting orbit $\bar{x}_{\mathbb{Z}}$ corresponds exactly to a quadratic turning point of the map $\Gamma(\cdot, \lambda)$ at the parameter $\lambda = \bar{\lambda}$.

In order to approximate a t-tangential connecting orbit, one needs exactly $p = t$ extra parameters in the system. In [Kleinkauf, 1998a; Kleinkauf, 1998b] the following defining system is used to approximate a nondegenerate t-tangential connecting orbit

$$\begin{array}{rcll} x_{n+1} - f(x_n, \lambda) & = & 0, & n = n_-, \cdots, n_+ - 1, \\ b(x_{n_-}, x_{n_+}, \lambda) & = & 0, & \\ \Phi_J(x_J, \lambda) & = & 0, & \end{array} \tag{3.3}$$

where $\Phi_J : S_J \times \mathbb{R}^p \to \mathbb{R}^t$ is a family of constraint functions.

A family of functions Φ_J is called **regular** at $(\bar{x}_{\mathbb{Z}}, \bar{\lambda})$ if the following three conditions are satisfied for some constants $C, N, \vartheta > 0$ and all $J = [n_-, n_+] \cap \mathbb{Z}$ with $|n_\pm| \geq N$.

(i) $\lim_{\min\{-n_-,n_+\}\to\infty} \Phi_J(\bar{x}_{|J},\bar{\lambda}) = 0$.

(ii) The $t\times t$–matrix $[D_x\Phi_J(\bar{x}_{|J},\bar{\lambda})(\bar{u}^1_{|J}),\ldots,D_x\Phi_J(\bar{x}_{|J},\bar{\lambda})(\bar{u}^t_{|J})]$ is nonsingular with uniformly bounded inverse

$$\left\| \left[D_x\Phi_J(\bar{x}_{|J},\bar{\lambda})(\bar{u}^1_{|J}),\ldots,D_x\Phi_J(\bar{x}_{|J},\bar{\lambda})(\bar{u}^t_{|J})\right]^{-1} \right\| \le C.$$

Here $\{\bar{u}^1_{\mathbb{Z}},\ldots,\bar{u}^t_{\mathbb{Z}}\}$ denotes some fixed basis of the t-dimensional null-space $\mathcal{N}(\Gamma_x(\bar{x}_{\mathbb{Z}},\bar{\lambda}))$.

(iii) The derivatives Φ'_J and Φ''_J are bounded in the closed ball $\|(x_J,\lambda)-(\bar{x}_{|J},\bar{\lambda})\|_\infty \le \vartheta$ uniformly in J.

To approximate quadratic nondegenerate 1-tangential connecting orbits we compute turning points of Eq. (2.3), which is equivalent to solve Eq. (3.3) with Φ_J defined as follows. Let

$$\Gamma_J : \begin{array}{ccc} S_J\times\mathbb{R}^1 & \to & S_J \\ (x_J,\lambda) & \mapsto & \big((x_{n+1}-f(x_n,\lambda))_{n\in\tilde{J}}, b(x_{n_-},x_{n_+},\lambda)\big), \end{array}$$

where $\tilde{J}=[n_-,n_+-1]\cap\mathbb{Z}$. Then a suitable constraint function Φ_J is

$$\Phi_J(x_J,\lambda) = \det\left(\frac{\partial}{\partial x_J}\Gamma_J(x_J,\lambda) - I\right),$$

where I is the identity matrix. For more details on defining equations and on test functions that are scalar but avoid determinants, see the surveys [Seydel, 1988; Govaerts, 2000; Beyn et al., 2002].

The linearization of Eq. (3.3) with respect to (x_J,λ) has the form of the matrix $\mathcal{M}$ in (1.7) and Newton's method can be implemented to solve the nonlinear Eq. (3.3).

Here we present a general approximation theorem for nondegenerate t-tangential connecting orbits that provides us with precise error estimates. The proofs are quite involved and carried out in [Kleinkauf, 1998a; Kleinkauf, 1998b].

Theorem 3.1 [Kleinkauf, 1998a, Theorem 3.5] *Assume $\bar{x}_{\mathbb{Z}}$ is a nondegenerate t-tangential connecting orbit. The boundary condition b of order (p_-,p_+) satisfies* (H5) *and Φ_J is regular. Then there exist constants $\delta, C, N>0$ such that for every $J=[n_-,n_+]\cap\mathbb{Z}$ with $|n_\pm|>N$, the* Eq. (3.3) *has a unique solution (x_J,λ_J) in the ball $\|x_J-\bar{x}_{|J}\|_\infty+|\lambda-\bar{\lambda}|<\delta$. The approximation error satisfies*

$$\|(x_J,\lambda_J)-(\bar{x}_{|J},\bar{\lambda})\|_\infty \le C\max\left\{\|b(\bar{x}_{n_-},\bar{x}_{n_+},\bar{\lambda}), \|\Phi_J(\bar{x}_{|J},\bar{\lambda})\|\right\}. \qquad (3.4)$$

Corollary 3.2 [Kleinkauf, 1998a, Corollary 3.7], [Kleinkauf, 1998c, Theorem 2.3] *Under the assumptions of* Theorem 3.1 *the following refined estimates hold:*

$$\|(x_J, \lambda_J) - (\bar{x}_{|J}, \bar{\lambda})\|_\infty \leq C \max \left\{ e^{p_- \sigma_{-u} n_-}, e^{-p_+ \sigma_{+s} n_+}, \|\Phi_J(\bar{x}_{|J}, \bar{\lambda})\| \right\}, \quad (3.5)$$

$$|\lambda_J - \bar{\lambda}| \leq C \left(e^{\sigma_{-s} n_-} + e^{-\sigma_{+u} n_+} \right) \left(e^{p_- \sigma_{-u} n_-} + e^{-p_+ \sigma_{+s} n_+} \right), \quad (3.6)$$

where $\sigma_{\pm u} > 1$ *is less than the smallest unstable eigenvalue at* $\xi_\pm$ *in absolutely value and* $0 < \sigma_{\pm s} < 1$ *is greater than the largest stable eigenvalue at* $\xi_\pm$ *in absolutely value.*

The estimate (3.6) shows that superconvergence occurs with respect to the parameter, a phenomenon that has been shown for ODE case in [Sandstede, 1997].

To illustrate the results numerically we compute 1-tangential connecting orbits for the Hénon map

$$f(x, y, \lambda_1, \lambda_2) = (1 + y - \lambda_1 x^2, \lambda_2 x). \quad (3.7)$$

For $\lambda_2 \neq 0$ the map $f(\cdot, \cdot, \lambda_1, \lambda_2)$ is C^∞–diffeomorphism and for $(\lambda_2 - 1)^2 > 4\lambda_1 \neq 0$ it has two families of fixed points $\xi_\pm(\lambda_1, \lambda_2) = (x_\pm, y_\pm)$ where

$$x_\pm = \frac{\lambda_2 - 1 \mp \sqrt{(\lambda_2 - 1)^2 + 4\lambda_1}}{2\lambda_1}, \quad y_\pm = \lambda_2 x_\pm. \quad (3.8)$$

Homoclinic tangency. We consider tangential homoclinic orbits associated to the fixed point $\xi_-(\lambda_1, \lambda_2)$.

Fixing $\bar{\lambda}_1 = 1.4$ and varying λ_2 near $\bar{\lambda}_2 = 0.3$, we get a branch of approximating homoclinic orbits. For the interval $J = [-25, 25]$ this branch of homoclinic orbits is shown in Fig. 3.1, where the amplitude of a numerical homoclinic orbit is defined as

$$\operatorname{amp}(x_J) = \sqrt{\sum_{n \in J} \|x_n - \xi_+\|^2}.$$

There are four turning points which correspond to quadratic 1-tangential homoclinic orbits. At these points the corresponding 1-tangential homoclinic orbits and at $\lambda_2 \approx 0.3$ a transversal homoclinic orbit are sketched by the relatively position and the shape of the unstable and stable manifolds.

We approximate a 1-tangential homoclinic orbit $x_{[-100,100]}$ at the parameter $\lambda_2 \approx 0.464527$ with $\operatorname{amp}(x_J) \approx 2.2446$. Parts of the numerical orbit

x_J together with parts of the corresponding invariant manifolds are shown in Fig. 3.2. This figure illustrates the tangential intersection of the invariant manifolds W_-^u and W_-^s along the homoclinic orbit x_J.

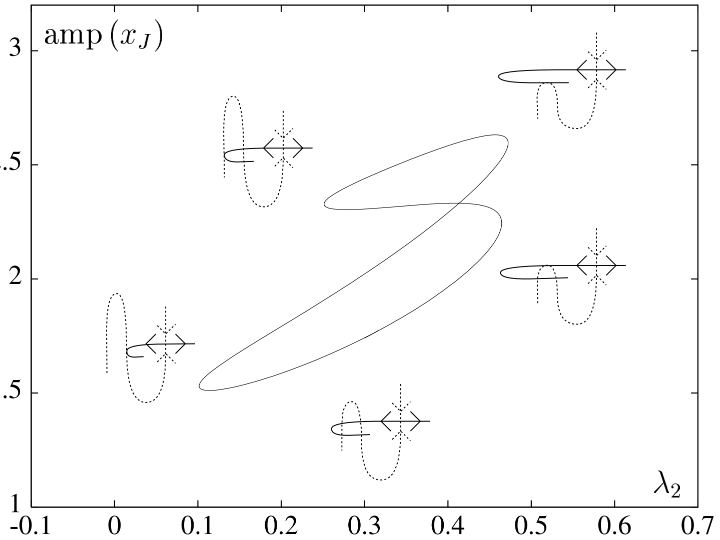

Figure 3.1: Branch of homoclinic orbits with a qualitative sketch of the unstable and the stable manifolds for the Hénon map.

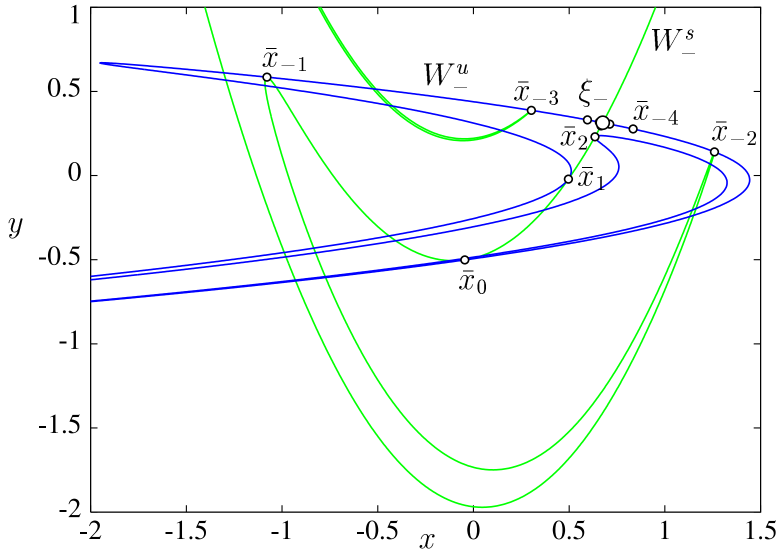

Figure 3.2: Parts of the numerical 1-tangential homoclinic orbit $\bar{x}_{[-100,100]}$ together with the corresponding unstable (blue) and stable (green) manifolds.

Heteroclinic tangency Fixing $\bar{\lambda}_1 = 1.4$ we calculate a quadratic 1-tangential heteroclinic orbit $x_{[-100,100]}$ at $\bar{\lambda}_2 \approx 0.31479$, which is shown in Fig. 3.3 together with the invariant manifolds W_-^u and W_+^s. This figure indicates the tangential intersection of the invariant manifolds W_-^u and W_+^s along the heteroclinic orbit x_J.

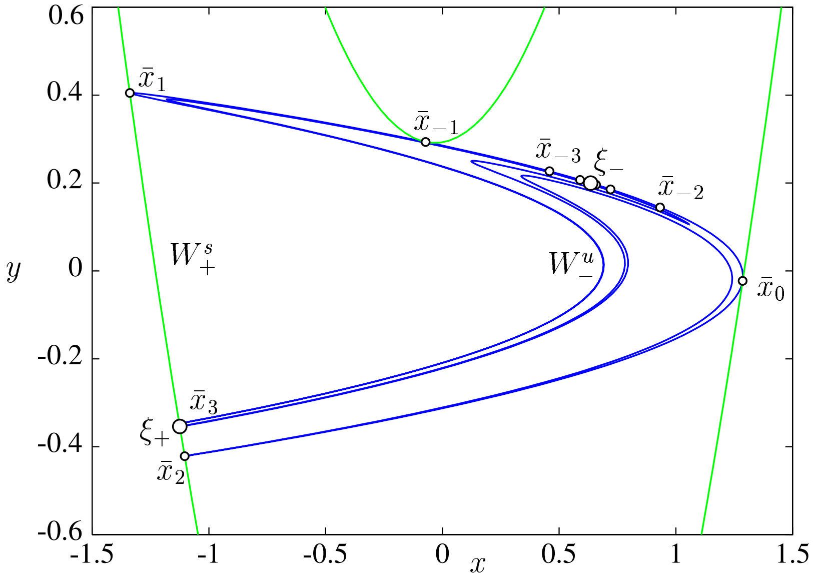

Figure 3.3: Parts of the numerical tangential heteroclinic orbit $\bar{x}_{[-100,100]}$ together with unstable (blue) and stable (green) manifolds.

3.2 Tangential fold-fold connecting orbit

In this subsection we show some numerical computations on 1-tangential fold-fold heteroclinic orbits for the implicit Euler method (2.10). In order to detect turning points, we use continuation techniques [Allgower & Georg, 1990] to trace a curve of transversal fold-fold heteroclinic orbits with respect to the parameter λ_2. In this way we locate 1-tangential fold-fold heteroclinic orbits. Define an amplitude of a numerical heteroclinic orbit as

$$\operatorname{amp}(x_J) = \min_{n \in J} \max \Big\{ \|x_n - \xi_-\|, \|x_n - \xi_+\| \Big\}.$$

Then the continuation picture shown in Fig. 2.8 is redisplayed in Fig. 3.4 in the coordinates of amplitude versus parameter λ_2 (the two corners appear due to the choice of a nonsmooth functional). Two turning points along this curve are obtained at $\bar{\lambda}_2^1 \approx 0.68481924468$ and $\bar{\lambda}_2^2 \approx 0.68481934446$ and they correspond to the two extremal λ-values in Fig. 2.8, respectively. At these two turning points, the fold-fold heteroclinic orbits are 1-tangential.

A numerical 1-tangential heteroclinic orbit at $\lambda_2 = \bar{\lambda}_2^2$ is shown in Fig. 3.5 and the tangential intersection of the corresponding manifolds is illustrated in Fig. 3.6 by numerical simulations.

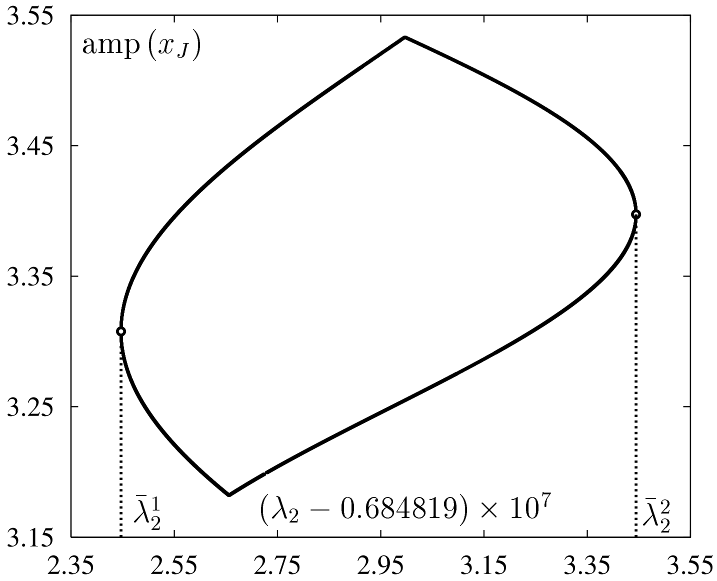

Figure 3.4: Continuation of a fold-fold heteroclinic orbit. With $\bar{\lambda}_2^1$ and $\bar{\lambda}_2^2$ we denote the corresponding turning points.

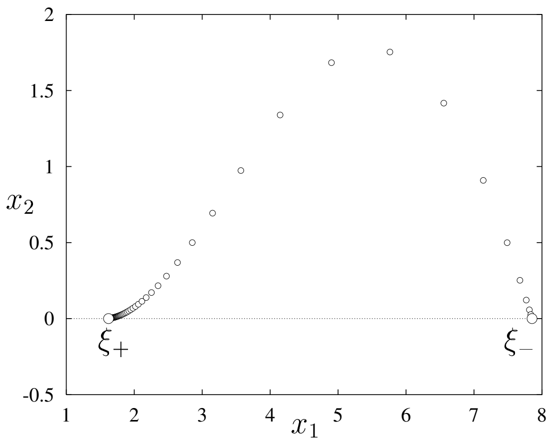

Figure 3.5: A numerical 1-tangential fold-fold heteroclinic orbit.

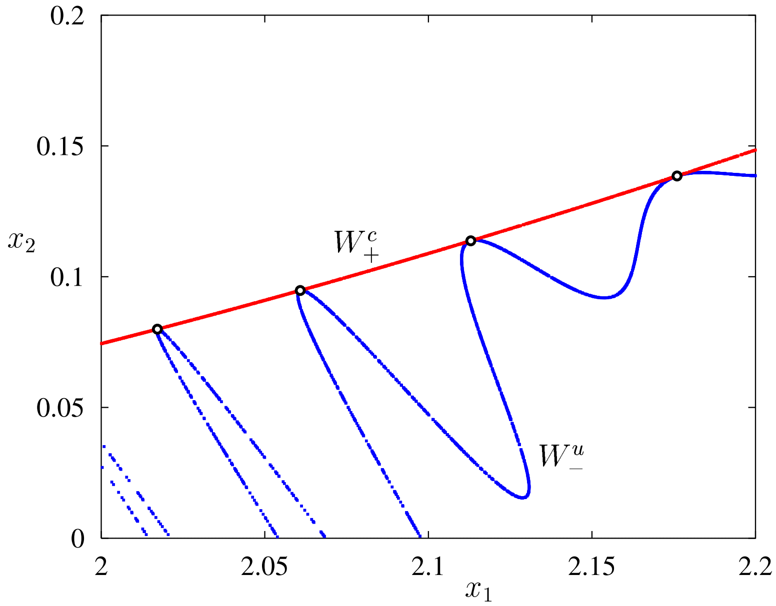

Figure 3.6: Tangential intersections of the unstable manifold W_-^u (blue) and the center manifold W_+^c (red) at the 1-tangential heteroclinic orbit $\bar{x}_J$.

4 Connecting orbit with positive index

In this section we study hyperbolic transversal connecting orbits with positive index. According to [Kleinkauf, 1998a; Kleinkauf, 1998b; Kleinkauf, 1998c] the algorithm (3.3) and error estimates in Theorem 3.1 apply to hyperbolic transversal connecting orbits with index 1.

For an illustration, we consider an extended Hénon map [Kleinkauf, 1998b; Kleinkauf, 1998c]

$$f(x, y, z, \lambda_1, \lambda_2, \lambda_3, \lambda_4) = \begin{pmatrix} 1 + y - \lambda_1 x^2 \\ \lambda_2 x \\ \lambda_3 xy + \lambda_4 y + ze^x \end{pmatrix}. \tag{4.1}$$

$f(\cdot, \cdot, \cdot, \lambda_1, \lambda_2, \lambda_3, \lambda_4)$ is a C^∞–diffeomorphism for $\lambda_2 \neq 0$. For $(\lambda_2 - 1)^2 > 4\lambda_1 \neq 0$ it has two fixed points $(x_\pm, y_\pm, z_\pm)$ where $(x_\pm, y_\pm)$ is defined in Eq. (3.8) and

$$z_\pm = \frac{\lambda_2\lambda_3 x_\pm + \lambda_2\lambda_4 x_\pm}{1 - e^{x_\pm}}.$$

It follows from the construction of the map f that each heteroclinic orbit $(\bar{x}_n, \bar{y}_n)_{n\in\mathbb{Z}}$ of the Hénon map (3.7) leads to a heteroclinic orbit $(\bar{x}_n, \bar{y}_n, 0)_{n\in\mathbb{Z}}$

of the extended Hénon map in case $\lambda_3 = \lambda_4 = 0$. Suppose an orbit $(\bar{x}_n, \bar{y}_n)_{n\in\mathbb{Z}}$ connects two fixed points (x_-, y_-) and (x_+, y_+) of the Hénon map (3.7) where each Jacobian at $(x_\pm, y_\pm)$ has one stable eigenvalue. Then the orbit $(\bar{x}_n, \bar{y}_n, 0)_{n\in\mathbb{Z}}$ connects the fixed points $(x_-, y_-, 0)$ and $(x_+, y_+, 0)$ of the extended Hénon map, and the Jacobian at $(x_-, y_-, 0)$ has two stable eigenvalues while the Jacobian at $(x_+, y_+, 0)$ still has one stable eigenvalue. This means that the orbit has index 1 and we need $p = 1$ extra parameter to approximate such a heteroclinic orbit.

Our goal is to compute an index 1 connection with λ_3 the parameter to be determined and the values $\lambda_4 = 1$, $\lambda_1 = 1.4$, $\lambda_2 = 0.4$ fixed. We start at $\lambda_4 = 0$ where we have $\lambda_3 = 0$ and the heteroclinic orbit form the Hénon map completed by an extra zero in the z-component. Then we employ continuation with respect to λ_4 and arrive at a solution (x_J, λ_3) for the extended Hénon map at $\lambda_3 \approx 1.1818$. Parts of the orbit x_J and parts of the unstable manifold W^u_- and stable manifold W^s_+ are shown in Fig. 4.1.

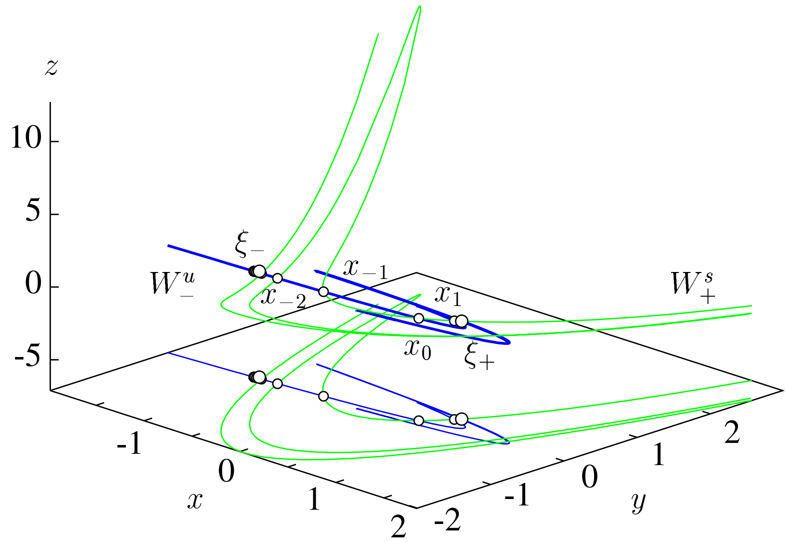

Figure 4.1: Parts of the one–dimensional manifolds W^u_- (blue) and W^s_+ (green) and the orbit $x_{[-100,100]}$ for the extended Hénon map. The orthogonal projection onto the (x, y)–plane is also shown.

References

Allgower, E. L. and Georg, K. [1990]. *Numerical continuation methods.* Springer-Verlag, Berlin. An introduction.

Arnold, V. I., Afraimovich, V., Ilyashenko, Y., and Shilnikov, L. P. [1994]. *Dynamical systems. V*, volume 5 of *Encyclopaedia of Mathematical Sciences.* Springer-Verlag, Berlin. Bifurcation theory and catastrophe theory, A translation of *Current problems in mathematics. Fundamental directions. Vol. 5 (Russian)*, Akad. Nauk SSSR, Vsesoyuz. Inst. Nauchn. i Tekhn. Inform., Moscow, 1986, Translation by N. D. Kazarinoff.

Bai, F. S., Spence, A., and Stuart, A. M. [1993]. The numerical computation of heteroclinic connections in systems of gradient partial differential equations. *SIAM J. Appl. Math.*, 53(3),743–769.

Beyn, W.-J. [1987]. The effect of discretization on homoclinic orbits. In *Bifurcation: analysis, algorithms, applications (Dortmund, 1986)*, volume 79 of *Internat. Schriftenreihe Numer. Math.*, pages 1–8. Birkhäuser, Basel.

Beyn, W.-J. [1990]. The numerical computation of connecting orbits in dynamical systems. *IMA J. Numer. Anal.*, 10,379–405.

Beyn, W.-J., Champneys, A., Doedel, E., Govaerts, W., Kuznetsov, Y. A., and Sandstede, B. [2002]. *Numerical continuation, and computation of normal forms*, volume 2 of *Handbook of dynamical systems.* North-Holland, Amsterdam.

Beyn, W.-J. and Kleinkauf, J.-M. [1997]. The numerical computation of homoclinic orbits for maps. *SIAM J. Numer. Anal.*, 34(3),1207–1236.

Champneys, A. R. and Kuznetsov, Y. A. [1994]. Numerical detection and continuation of codimension-two homoclinic bifurcations. *Internat. J. Bifur. Chaos Appl. Sci. Engrg.*, 4(4),785–822.

Doedel, E. J. and Friedman, M. J. [1989]. Numerical computation of heteroclinic orbits. Continuation techniques and bifurcation problems. *J. Comput. Appl. Math.*, 26(1-2),155–170.

Fiedler, B. and Scheurle, J. [1996]. Discretization of homoclinic orbits, rapid forcing and "invisible" chaos. *Mem. Amer. Math. Soc.*, 119(570),viii+79.

Friedman, M. J. and Doedel, E. J. [1991]. Numerical computation and continuation of invariant manifolds connecting fixed points. *SIAM J. Numer. Anal.*, 28(3),789–808.

Friedman, M. J. and Doedel, E. J. [1993]. Computational methods for global analysis of homoclinic and heteroclinic orbits: a case study. *J. Dynam. Differential Equations*, 5(1),37–57.

Govaerts, W. [2000]. *Numerical methods for bifurcations of dynamical equilibria*. Society for Industrial and Applied Mathematics (SIAM), Philadelphia.

Hager, W. W. [1988]. *Applied numerical linear algebra*. Prentice Hall, Englewood Cliffs, New Jersey.

Hale, J. K. and Koçak, H. [1991]. *Dynamics and bifurcations*, volume 3 of *Texts in Applied Mathematics*. Springer-Verlag, New York.

Hale, J. K. and Lin, X. B. [1986]. Symbolic dynamics and nonlinear semiflows. *Ann. Mat. Pura Appl.*, 144(4),229–259.

Hüls, T. [1998]. Heterokline Orbits in diskreten dynamischen Systemen. Master's thesis, Universität Bielefeld.

Hüls, T. [2003]. A model function for polynomial rates in discrete dynamical systems. Technical Report 03-007, Institute of Mathmatics, University of Bielefeld. Applied Mathematics Letters (to appear).

Hüls, T. [2003]. *Numerische Approximation nicht-hyperbolischer heterokliner Orbits*. PhD thesis, Universität Bielefeld. Shaker Verlag, Aachen.

Hüls, T. and Zou, Y. [2001]. Polynomial estimates and discrete saddle-node homoclinic orbits. *J. Math. Anal. Appl.*, 256(1),115–126.

Kleinkauf, J.-M. [1994]. Numerische Berechnung diskreter homokliner Orbits. Master's thesis, Universität Bielefeld.

Kleinkauf, J.-M. [1998a]. The numerical computation and geometrical analysis of heteroclinic tangencies. Technical Report 98-048, SFB 343. http://www.mathematik.uni-bielefeld.de/sfb343/preprints.

Kleinkauf, J.-M. [1998b]. *Numerische Analyse tangentialer homokliner Orbits*. PhD thesis, Universität Bielefeld. Shaker Verlag, Aachen.

Kleinkauf, J.-M. [1998c]. Superconvergence estimates for the numerical computation of heteroclinics for maps. Technical Report 98-052, SFB 343. http://www.mathematik.uni-bielefeld.de/sfb343/preprints.

Krauskopf, B. and Osinga, H. [1998]. Globalizing two-dimensional unstable manifolds of maps. *Internat. J. Bifur. Chaos Appl. Sci. Engrg.*, 8(3),483–503.

Kuznetsov, Y. A. [1998]. *Elements of applied bifurcation theory.* Springer-Verlag, New York, second edition.

Kuznetsov, Y. A. and Levitin, V. V. [1998]. CONTENT – integrated environment for analysis of dynamical systems. http://www.cwi.nl/ftp/CONTENT.

Lani-Wayda, B. [1995]. *Hyperbolic sets, shadowing and persistence for non-invertible mappings in Banach spaces*, volume 334 of *Pitman Research Notes in Mathematics Series.* Longman, Harlow.

Mallet-Paret, J. and Sell, G. R. [1987]. *The principle of spatial averaging and inertial manifolds for reaction-diffusion equation.* Springer, Berlin. Lecture Notes in Mathematics, 1248.

Mel'nikov, V. K. [1963]. On the stability of a center for time-periodic perturbations. (russian). *Trans. Moscow Math. Soc.*, 12,3–52.

Newhouse, S., Palis, J., and Takens, F. [1983]. Bifurcations and stability of families of diffeomorphisms. *Inst. Hautes Études Sci. Publ. Math.*, 57,5–71.

Palis, J. and Takens, F. [1993]. *Hyperbolicity and sensitive chaotic dynamics at homoclinic bifurcations*, volume 35 of *Cambridge Studies in Advanced Mathematics.* Cambridge University Press, Cambridge. Fractal dimensions and infinitely many attractors.

Palmer, K. J. [1988]. Exponential dichotomies, the shadowing lemma and transversal homoclinic points. In *Dynamics reported, Vol. 1*, pages 265–306. Teubner, Stuttgart.

Sandstede, B. [1997]. Convergence estimates for the numerical approximation of homoclinic solutions. *IMA J. Numer. Anal.*, 17(3),437–462.

Schecter, S. [1993]. Numerical computation of saddle-node homoclinic bifurcation points. *SIAM J. Numer. Anal.*, 30(4),1155–1178.

Schecter, S. [1995]. Rate of convergence of numerical approximations to homoclinic bifurcation points. *IMA J. Numer. Anal.*, 15(1),23–60.

Seydel, R. [1979]. Numerical computation of branch points of ordinary differential equations. *Numer. Math.*, 32(1),51–68.

Seydel, R. [1988]. *From equilibrium to chaos.* Elsevier, New York. Practical bifurcation and stability analysis.

Smale, S. [1963]. Diffeomorphisms with many periodic points. In *Differential and Combinatorial Topology,* Cairns, S.S. (ed.), pages 63–80. Princeton Univ. Press, Princeton, N.J.

Steinlein, H. and Walther, H.-O. [1990]. Hyperbolic sets, transversal homoclinic trajectories, and symbolic dynamics for C^1-maps in Banach spaces. *J. Dynam. Differential Equations*, 2(3),325–365.

Wiggins, S. [1988]. *Global bifurcations and chaos: Analytical methods.*, volume 73 of *Applied Mathematical Sciences.* Springer-Verlag, New York.

Wiggins, S. [1990]. *Introduction to applied nonlinear dynamical systems and chaos.* Springer-Verlag, New York.

Zou, Y.-K. and Beyn, W.-J. [1996]. Discretizations of dynamical systems with a saddle-node homoclinic orbit. *Discrete Contin. Dynam. Systems*, 2(3),351–365.

Zou, Y.-K. and Beyn, W.-J. [2003]. On manifolds of connecting orbits in discretizations of dynamical systems. *Nonlinear Anal. TMA*, 52(5),1499–1520.